Boundary Conditions for- Single-Ion Diffusion

Pete McGill and Mark F. Schumaker
Department of Pure and Applied Mathematics, Washington State University, Pullman, Washington 99164-3113 USA

ABSTRACT We have constructed a theory for diffusion through the pore of a single-ion channel by taking a limit of a random walk around a cycle of states. Similar to Levitt's theory of single-ion diffusion, one obtains boundary conditions for the Nernst-Planck equation that guarantee that the pore is occupied by at most one ion. Two of the terms in the boundary conditions are identical to those given by Levitt. However, the construction gives rise to a third term not found in Levitt's theory. With this term, the channel spends exponentially distributed intervals in the empty state. Ion sample paths have been simulated to help visualize trajectories near the channel entrances, with and without the new term. We use the modified Levitt theory to fit several potential profiles to the conductance data of Russell et al. In particular, we have analyzed the profile for Na^+ in gramicidin calculated by Roux and Karplus. The peak-to-peak amplitude of their result must be reduced to at most 35% of its original value to fit the data. But with this reduction, excellent fits are obtained.

GLOSSARY

When uppercase and lowercase symbols are given together, lowercase denotes dimensionless quantities. Subscripts or superscripts $s \in \{a, b\}$ distinguish random walk cycles in the Methods, and both cycles and ion species in Appendix C.

Nomenclature

A, $A(x)$, A_i	Pore cross-section. $A_i = A(x_i)$
$C(x)$, C_i, C_s, C_i^s	Ion concentration in pore. $C_i = C(x_i)$
C_I, C_{II}, C_I^s, C_{II}^s	Permeant ion concentration in solution on sides I or II
C_b	Common value of C_I and C_{II}
C_{eff}	Effective permeant ion concentration outside channel entrance
D, $D(x)$ D_i, D_s	Diffusion coefficient in pore. $D_i = D(x_i)$
D_{eff}	Effective diffusion coefficient outside channel entrance
e_0	Elementary electrical charge
f, F	Denominators of J defined by Eqs. 26 and 77
G_0	Conductance at symmetrical equilibrium
$h(x)$, $H(x)$	Refer to integrals defined in Eq. 22 or 72
$\mathcal{I}$	Electrical current through channel
J, J_s	Ion flux through pore
K_M	Michaelis constant of G_0 as a function of C_b
k	Boltzmann's constant
L	Length of pore
n	Number of random walk sites across pore interior
n'	Flux ratio exponent
P_E	Probability that the pore is not occupied by an ion
P_{enter}	Probability of entering channel from random walk empty state
P_i, P_i^s	Probability of random walk state i or i_s
$\mathcal{P}$	One-dimensional probability density inside pore
$p_{MLT}(t)$	Probability that an empty state interval in the modified Levitt theory will have length of at least t
r_c	Capture radius
T	Absolute temperature
$\bar{T}_{Levitt}$	Mean time in empty state of random walks converging to Levitt theory
$\bar{T}_{MLT}$	Mean time in empty state of random walks converging to modified Levitt theory
t,Δt	Time. Random walk time step
$U(\xi)$	Free energy profile for Na^+ in gramicidin given by Roux and Karplus (1993) or Åqvist and Warshel (1989)
v, v_s	Total potential energy of ion (see Eq. 2)
v', v'_i, $v_i^{s\prime}$	$v' = dv/dx$, $v'_i = v'(x_i)$
w	Entrance width defined for JCJ profile
X, x, x_i	Distance along pore axis. $x_i = i/n$
z	Ion valence

Greek symbols

$\alpha_i C_I$, $\alpha_{II} C_{II}$	Entrance transition probabilities on sides I and II
β_I, β_{II}	Exit transition probabilities on sides I and II
γ_i	Probability of transition from state i to $i + 1$
$\hat{\gamma}_i$	Probability of transition from state i to $i - 1$
ϵ	Well depth (see Fig. 1)
ζ	Common value of entrance potential, $\phi(0) = \phi(1) = \zeta$
η	barrier height (see Fig. 1)
κ_I, κ_{II}, κ	Binding kinetics parameters on side I or II, and their common value
$\Delta\mu$	Dimensionless chemical potential difference across membrane
ξ	Axial distance from channel center
ξ_{max}	Half-width of single-file region
σ	Potential profile coefficient, defined by Eq. 57
$\Delta\tau$	A fixed time interval, independent of n
$\Phi(x)$, $\phi(x)$, $\phi_s(x)$	Intrinsic potential energy in pore interior
$\bar{\Phi}$, $\bar{\phi}$	Average value of Φ or ϕ (see Eq. 54)
Φ_{expt}	Experimental value of $\bar{\Phi}$
$\Psi(x)$, $\psi(x)$	Applied electrical potential in pore interior
Ψ_R	Reversal potential
ψ_I, ψ_{II}	Electrical potential of solution on side I or II

Received for publication 14 August 1995 and in final form 24 June 1996.
Address reprint requests to Dr. Mark F. Schumaker, Department of Pure and Applied Mathematics, Washington State University, Pullman, WA 99164-3113. Tel.: 509-335-3170; 509-335-1188; E-mail: schumaker@beta.math.wsu.edu.

0006-3495/96/10/1723/20 $2.00

INTRODUCTION

Our knowledge of the structure and function of many ion channels suggests that their permeation pores often have narrow regions that can be occupied by only one or a few

permeant ions at any one time (for a general review, see Hille, 1992). Gramicidin is an especially simple and well-characterized channel, with a permeation pore that has room for about 10 water molecules in single file. Only one or two permeant ions can occupy the pore at one time. With such restricted geometries, occupancy constraints are an important feature of models that attempt to describe ion permeation through these channels.

Occupancy constraints are built into discrete-state models of ion permeation (for example, Läuger, 1973; Hille and Schwarz, 1978). Unfortunately, the description of ion transport provided by these models is only accurate under special circumstances (Cooper et al., 1985, 1988; Dani and Levitt, 1990). Diffusion models of permeation are more generally applicable. This paper is concerned with the description of single-ion diffusion, where only a single ion can occupy the pore at one time.

Levitt (1986) made a major contribution toward solving this problem. He found boundary conditions for the Nernst-Planck equation that result in a diffusion involving at most a single ion. Given the potential energy of the ion as a function of its location on a channel axis, Levitt's theory provides a description of single-ion permeation through the channel. Jakobsson and Chiu (1987) and Chiu and Jakobsson (1989) subsequently showed that the gramicidin conductance data of Russell et al. (1986) can be fit by Levitt's theory using a plausible model for the gramicidin potential profile.

In Methods and Appendix A we present a new derivation of Levitt's single-ion diffusion theory. We construct a random walk with n sites distributed along the pore and a single empty state. By choosing transition probabilities appropriately, we obtain precisely Levitt's original theory on taking the limit $n \to \infty$. The new construction has the advantage that we are able to study in detail the nature of the ion trajectories at the channel entrances. In particular, we calculate the distribution of empty state dwell times underlying our representation of Levitt's theory. Surprisingly, the ion trajectories have zero mean dwell time in the empty state, even though the empty state has positive probability! In Results and Fig. 4, we explain how this is possible.

We believe this unphysical result emphasizes the necessity of modifying the boundary conditions given by Levitt (1986). One approach has already been given by Chiu and Jakobsson (1989). They added access resistance to Levitt's theory, using the mathematical form of resistances in series. However, this approach requires that a number of assumptions are made about how ions flow to and from the channel entrances.

The random walk construction suggests an alternative way to modify the Levitt boundary conditions. By changing the way ion entrance and exit rates scale with n, a new term appears in the boundary conditions that is not found in Levitt's theory. The empty state dwell times of this new modified Levitt theory are exponentially distributed with positive mean. This is the same distribution of dwell times that underlies discrete-state (rate theory) descriptions of ion permeation, and we will argue that it approximates reality well if certain plausible assumptions are satisfied.

Similar to the effect of adding access resistance to Levitt's theory, the new term in the modified theory boundary conditions decreases the conductance. However, compared with adding access resistance, the modified theory has the advantage of simplicity. Only two new parameters are needed to describe ion entrance and exit, one for each pore entrance. In the case of a symmetrical channel like gramicidin, the two new parameters are reduced to one, which may be considered the mean dwell time in the empty state.

Our random walk construction also leads to a new technique for simulating ion trajectories. Because the construction employs finite-state random walks converging to a diffusion, we only need to simulate the random walks for large but finite n to obtain a simulation procedure with a well-characterized relationship to the diffusion theory. In particular, there is a clear procedure for introducing ions into the pore from the channel entrances. Previous Brownian dynamics simulations (Cooper et al., 1985; Jakobsson and Chiu, 1987) have employed a heuristic device, the "entrance tube," to introduce ions into the pore from the channel entrances.

Following the lead of Jakobsson and Chiu (1987), we use our theory as a bridge between theoretical calculations of ion free energies and experiment. The Results section discusses three different free energy profiles for Na^+ in gramicidin, that of Jordan (1982) and Jakobsson and Chiu (1987), as well as those of Åqvist and Warshel (1989) and Roux and Karplus (1993). We use the modified Levitt theory to fit these to the Na^+ conductance data of Russell et al. (1986). The profile from the group of Roux and Karplus is the result of a relatively recent molecular dynamics calculation. We find that its peak-to-peak amplitude must be reduced to at most 35% of its original value to fit the data. But with this reduction, excellent fits are obtained.

THE MODIFIED LEVITT THEORY

We now recall the Nernst-Planck equation, introducing our terminology, and give the central mathematical result of this paper.

The Nernst-Planck equation (see, for example, Hille, 1992) describes time-independent diffusion in one spatial dimension. We write it in the form

$$J = -\frac{AD}{L}\left(\frac{dC}{dx} + v'C\right), \tag{1}$$

where A is a pore cross section, D is the diffusion coefficient of the ion-water contents of the channel, and L is the length of the pore. Let X denote the distance along the axis of the pore; then the dimensionless coordinate $x = X/L$ has value $x = 0$ at the channel entrance on side I and $x = 1$ on side II. In the following, A and D are assumed to be constant, but Appendix B generalizes the discussion to consider $A(x)$ and $D(x)$. $C(x)$ is the ion concentration within the pore; $AC(x)$

can be regarded as a probability density per unit length. The constant J is the ion flux through the pore. $v(x)$ is the dimensionless total potential energy of an ion at coordinate x in the pore, and it is the sum of two terms,

$$v(x) = \phi(x) + \psi(x). \tag{2}$$

$v'(x)$ is the derivative of $v(x)$. Let $\Phi(x)$ be the intrinsic electrochemical potential energy of the ion's interaction with the channel-membrane system; then $\phi(x) = \Phi(x)/kT$. A voltage difference may also be applied across the channel, and we will use the convention that the voltage on side I is Ψ_I and that on side II is zero. The resulting electrical potential energy of the ion in the pore can be expressed in dimensionless form as $\psi(x) = ze_0\Psi(x)/kT$, where z is the ion valence, e_0 is the elementary electrical charge, k is Boltzmann's constant, and T is the absolute temperature. Fig. 1 sketches the relationship between Φ, Ψ, and the pore.

Levitt's (1986) single-ion boundary conditions for the Nernst-Planck equation are

$$C(0) = P_E e^{\psi_I - v(0)} C_I, \tag{3}$$

$$C(1) = P_E e^{-v(1)} C_{II}. \tag{4}$$

The Nernst-Planck equation is of first order, and the two boundary conditions specify the value of J as well as the constant of integration. We will refer to the single-ion diffusion theory that satisfies these boundary conditions as the Levitt theory. In these equations, C_I and C_{II} are the bulk concentrations of the permeant ion on sides I and II of the membrane (the question of whether to interpret C_I and C_{II} as concentrations or activities is addressed in the Discussion section). $C(0)$ and $C(1)$ are the pore ion concentrations at the channel entrances. P_E is the probability that the channel is not occupied by an ion. $v(0)$ and $v(1)$ are values of the total potential at the channel entrances.

In Methods we model single ions in a membrane channel by means of a random walk around a cycle of states, shown in Fig. 2 *A*. There are $n + 1$ states in the cycle. The permeation pore corresponds to states 1 through n across the top. The state E represents an empty channel, occupied only by water. We take the limit as $n \to \infty$, obtaining a diffusion process on an interval, with transitions between the end

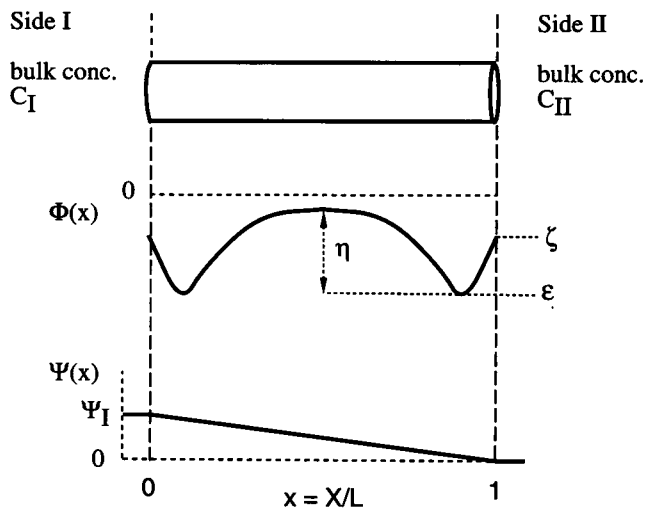

FIGURE 1 Sketch of the relationship between the ion channel pore, the intrinsic potential Φ, and the applied potential Ψ. These sketches are consistent with the simplifying assumptions described at the beginning of Results. Φ is characterized by entrance potential ζ, well energy ϵ, and barrier height η.

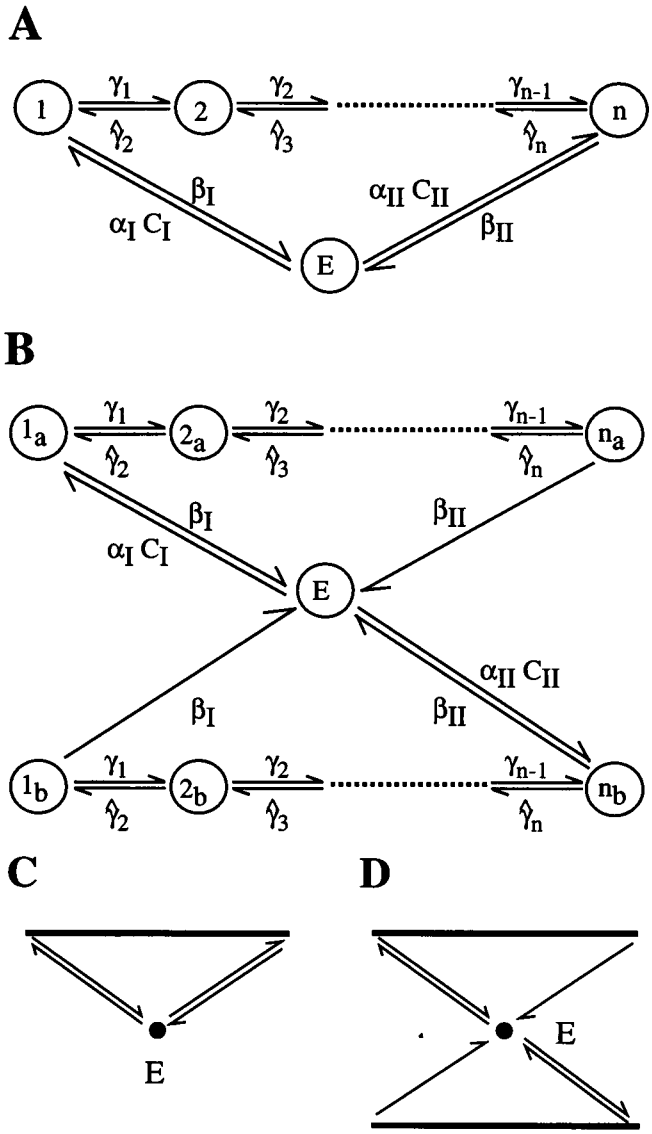

FIGURE 2 State diagrams of Levitt and modified Levitt theories. (*A*) One-cycle random walk and transition probabilities. *E* represents the empty channel state. State i, $0 \le i \le n$, represents an ion at location $x_i = i/n$ within the pore. (*B*) Directed two-cycle random walk and transition probabilities. Cycle *a* is occupied by ions that enter the channel from side I, and cycle *b* is occupied by ions that enter the channel from side II. (*C*) One-cycle continuous-state diagram. This is obtained as the $n \to \infty$ limit of the one-cycle random walk. *E* represents the empty state, and each point on the remainder of the diagram represents an ion location in the pore. (*D*) Directed two-cycle continuous-state diagram. This is obtained as the $n \to \infty$ limit of the directed two-cycle random walk.

points and the empty state (see Fig. 2 *C*). When transition probabilities that describe the random walk are chosen appropriately, the Nernst-Planck equation (Eq. 1) describes the diffusion in the interior of the pore.

In the random walk, we find two different ways to scale the rate of ion entrance into the pore with n. One of these leads to Levitt's original boundary conditions (Eqs. 3 and 4) is discussed in Appendix A. The second scaling procedure, used in Methods, gives rise to a third term in each equation

$$C(0) - P_E e^{\psi_1 - v(0)} C_I + \kappa_I (L/AD) J = 0, \quad (5)$$

$$C(1) - P_E e^{-v(1)} C_{II} - \kappa_{II} (L/AD) J = 0. \quad (6)$$

The additional terms are proportional to the ion flux J and two new factors κ_I and κ_{II}. We call these latter quantities binding kinetics parameters; they help to specify the ion entrance rates at each end of the pore. The Nernst-Planck equation, together with these boundary conditions, is the modified Levitt theory.

METHODS

Modified Levitt theory for one permeant ion

Fig. 2 *A* diagrams a discrete-time, discrete-state random walk (e.g., Chandrasekhar, 1943; Reif, 1965; Karlin and Taylor, 1981). This random walk incorporates the single-ion occupancy constraint by construction, in a manner similar to that of a single-ion rate theory (Läuger, 1973). However, the states 1 through n should not be interpreted as ion binding sites in the sense of rate theory. Transition probabilities will be defined in a different way. The purpose of this construction is to obtain the Nernst-Planck equation and appropriate boundary conditions in the limit $n \to \infty$.

Let P_i be the probability of state i. If each of the n states represents an equal part of the total channel volume AL, we can write the following relationship between the state probability and ion concentration $C_i = C(x_i)$:

$$P_i = C_i AL/n. \quad (7)$$

Transition probabilities between the channel states are denoted γ_i for transitions to the right and $\hat{\gamma}_i$ for transitions to the left. Suppose state i is occupied at time t, where $2 \le i \le n - 1$, and let Δt be the time step. Then at time $t + \Delta t$, state $i - 1$ will be occupied with probability $\hat{\gamma}_i$, state $i + 1$ will be occupied with probability γ_i, and state i will be occupied with probability $1 - \gamma_i - \hat{\gamma}_i$. Transitions to state E can be made from states 1 and n with exit transition probabilities β_I and β_{II}, respectively. Transitions from the empty state to channel entrance states 1 or n are made with transition probabilities $\alpha_I C_I$ and $\alpha_{II} C_{II}$, respectively.

The Nernst-Planck equation (Eq. 1) will be obtained when the transition probabilities are related to the physical parameters of the problem using the following definitions:

$$\gamma_i = \Delta t DL^{-2}(n^2 - nv_i'/2), \quad (8)$$

$$\hat{\gamma}_i = \Delta t DL^{-2}(n^2 + nv_i'/2), \quad (9)$$

$$\alpha_I = \Delta t ADL^{-1} \kappa_I^{-1} e^{\psi_1 - v(0)}, \quad (10)$$

$$\alpha_{II} = \Delta t ADL^{-1} \kappa_{II}^{-1} e^{-v(1)}, \quad (11)$$

$$\beta_I = \Delta t DL^{-2} n \kappa_I^{-1}, \quad (12)$$

$$\beta_{II} = \Delta t DL^{-2} n \kappa_{II}^{-1}. \quad (13)$$

Factors of A, D, and L in these definitions are specified in part by the requirement that the transition probabilities be dimensionless.

These probabilities are all proportional to the time step Δt. Suppose the system is in any state i at time t. The sum of the transition probabilities for leaving state i at the next time step must be no greater than 1, and this must remain true as $n \to \infty$. The required relationship will hold if we specify

$$\Delta t = \Delta \tau / n^2. \quad (14)$$

with $\Delta \tau$ independent of n and chosen appropriately.

The probabilities γ_i and $\hat{\gamma}_i$ each involve two terms. Terms proportional to n^2 give a diffusive contribution to the Nernst-Planck equation, and those proportional to n give a systematic contribution. Notice that these latter terms are also proportional to v', the derivative of the total potential, reflecting a force acting on the ion. Perhaps it is not surprising that the diffusive terms, which make the same contribution to γ_i and $\hat{\gamma}_i$, must scale as a higher power of n than the systematic terms, which make opposite contributions, to give comparable effects in the limit $n \to \infty$. This will be seen when the limit is taken below.

The entrance and exit rates at the channel entrance on side I are constrained by the thermodynamic requirement that, at equilibrium,

$$P_1/P_E = \alpha_I C_I/\beta_I = (LA/n) C_I e^{\psi_1 - v(0)}. \quad (15)$$

The right-hand side is the product of the channel volume associated with state 1, the bulk permeant ion concentration on side I, and a Boltzmann factor that takes into account the free energy difference between an ion in the bulk and at the channel entrance. However, α_I and β_I may be multiplied by an arbitrary common factor and remain consistent with thermodynamics. This degree of freedom is the binding kinetics parameter κ_I^{-1} in Eqs. 10 and 12, and contains information about the ion entrance and exit processes. For example, the expressions for the entrance and exit rate constants given are proportional to the diffusion coefficient D of the ion in the channel. A different effective diffusion coefficient may be more appropriate, contributing a factor to κ.

Under steady-state conditions, the probability of making a transition into any state must equal the probability of leaving it. This requirement leads to the following equations:

$$P_i(\gamma_i + \hat{\gamma}_i) = P_{i-1}\gamma_{i-1} + P_{i+1}\hat{\gamma}_{i+1}, \quad (16)$$

$$P_1(\gamma_1 + \beta_I) = P_2\hat{\gamma}_2 + P_E\alpha_I C_I, \quad (17)$$

$$P_n(\hat{\gamma}_n + \beta_{II}) = P_{n-1}\gamma_{n-1} + P_E\alpha_{II} C_{II}. \quad (18)$$

The first of these applies for $2 \leq i \leq n-1$. Using the language of chemical kinetics, these equations are analogous to those that would be obtained from the condition that a network of first-order reactions is at steady state. The difference is that, in the present case, time is discrete.

On taking $n \to \infty$, Eq. 16 will lead to a differential equation describing transport of ions through the interior of the channel. Equations 17 and 18 will give the boundary conditions for the transport equation.

We first consider transport in the interior of the channel. Substituting Eqs. 7, 8, and 9 into Eq. 16, multiplying by a common factor, and collecting terms on the left, we obtain

$$n^2(C_{i+1} - 2C_i + C_{i-1}) + \frac{n}{2}(C_{i+1}v'_{i+1} - C_{i-1}v'_{i-1}) = 0. \tag{19}$$

Recalling that $C_i = C(x_i) = C(i/n)$, we recognize a finite-difference approximation of the second derivative of C and, similarly, a symmetrical finite difference approximation of the first derivative of Cv'. Letting $n \to \infty$ and $i \to \infty$, so that their ratio $i/n \to x$, we obtain

$$\frac{AD}{L}\left(\frac{d^2C}{dx^2} + \frac{d}{dx}v'C\right) = 0. \tag{20}$$

We have reintroduced a physical combination of factors that helps us recognize this as a generalized diffusion equation, the time-independent Fokker-Planck equation (e.g., Karlin and Taylor, 1981; Gardiner, 1983; Risken, 1989). The first term is diffusive and the second corresponds to a systematic force on the diffuser that is proportional to $-v'$. Integrating once, we obtain the Nernst-Planck equation (Eq. 1), where the constant of integration is the ion flux J. We multiply Eq. 1 by the integrating factor $\exp[v(x)]$ and integrate again, obtaining

$$Jh(x) = -ADL^{-1}[C(x)e^{v(x)} - C(0)e^{v(0)}], \tag{21}$$

where

$$h(x) = \int_0^x e^{v(x')}dx'. \tag{22}$$

The constants of integration, J and $C(0)e^{v(0)}$, must now be determined by application of boundary conditions, which we develop next.

Consider the boundary on side I. Substituting Eqs. 7–10 and 12 into Eq. 17 and dividing by a common factor, we obtain

$$n(C_2 - C_1) + \frac{1}{2}(C_1v'_1 + C_2v'_2) + (P_EC_Ie^{\psi_I - v(0)} - C_1)\kappa_I^{-1} = 0. \tag{23}$$

Letting $n \to \infty$ then gives

$$C(0) - P_EC_Ie^{\psi_I - v(0)} - \kappa_I[C'(0) + C(0)v'(0)] = 0. \tag{24}$$

Making use of Eq. 1, we finally have the boundary condition on side I, Eq. 5. A similar analysis, beginning with the steady-state condition of Eq. 18, yields the boundary condition on side II, Eq. 6.

We now have the Nernst-Planck equation (Eq. 1) and boundary conditions (Eqs. 5 and 6), which guarantee single-ion diffusion. These boundary conditions are somewhat unusual in that they depend on P_E, which itself depends on the solution! However, Levitt (1986) has demonstrated that the solution can be easily obtained.

We next find a formula for the current J. We combine the boundary conditions, Eqs. 5 and 6, to obtain an expression for $C(1)\exp v(1) - C(0)\exp v(0)$, and substitute this into the result of evaluating Eq. 21 at $x = 1$. Solving for J, we obtain

$$J = P_E(AD/L)[C_Ie^{\psi_I} - C_{II}]f^{-1}, \tag{25}$$

where

$$f = \kappa_Ie^{v(0)} + \kappa_{II}e^{v(1)} + h(1). \tag{26}$$

P_E remains to be determined. Starting from Eq. 21, we eliminate the integration constants by using Eq. 5 to substitute for $C(0)\exp v(0)$ and Eq. 25 to substitute for J. Solving the resultant expression for $C(x)$, we obtain

$$C(x) = P_Ee^{-v(x)}[C_Ie^{\psi_I} - (C_Ie^{\psi_I} - C_{II})(\kappa_Ie^{v(0)} + h(x))f^{-1}]. \tag{27}$$

The probability that the channel is empty is then given by

$$\begin{aligned} P_E &= 1 - \int_0^1 ALC(x)dx \\ &= 1 - P_E\left[C_Ie^{\psi_I}\int_0^1 ALe^{-v(x)}dx + (C_{II} - C_Ie^{\psi_I})R\right], \end{aligned} \tag{28}$$

where

$$R = \int_0^1 ALe^{-v(x)}(\kappa_Ie^{v(0)} + h(x))f^{-1}dx. \tag{29}$$

Now we simply solve Eq. 28 for P_E:

$$P_E = \left(1 + C_Ie^{\psi_I}\int_0^1 ALe^{-v(x)}dx + (C_{II} - C_Ie^{\psi_I})R\right)^{-1}. \tag{30}$$

With this result, Eq. 25 provides a solution for J and Eq. 27 gives $C(x)$.

In summary, the limiting process takes a sequence of discrete-state random walks, the nth member of which is depicted in Fig. 2 *A*, to a diffusion process on a continuous-state diagram with one cycle, shown in Fig. 2 *C*. The cycle is parameterized by a coordinate x, the value of which may be regarded as the position of the ion. However, the state x really refers to the configuration of the whole channel system, including the interaction with its environment.

The solution of this modified Levitt theory depends on κ_I and κ_{II}. Levitt's theory (1986) corresponds to the limits $\kappa_I \to 0$ and $\kappa_{II} \to 0$. It can also be obtained by a different scaling of the entrance and exit transition probabilities with respect to n. Appendix A sketches this more direct derivation.

Derivation of the modified Levitt theory using a directed two-cycle random walk

In this section we will give an alternative derivation of the modified Levitt theory for one permeant ion. It will lead to the same results as obtained in the last section; the difference is that we will now make a distinction between ions that enter the channel from side I and those that enter the channel from side II. These ions are assumed to be chemically identical.

The alternative derivation proves useful in two ways. First, unidirectional ion fluxes emerge naturally from the analysis. These are required for the calculation of the flux ratio exponent. Second, the two-cycle random walk is a very convenient basis for numerical simulations, which we shall describe in the next section.

Consider the random walk shown in Fig. 2 *B*. There are two cycles, linked by a common empty state E. Cycle a has states labeled i_a, with $1 \le i \le n$. It is occupied by ions that enter the channel from side I and leave from either side. There is an irreversible transition from state n_a on side II to the empty state. Cycle b has states labeled i_b, $1 \le i \le n$. It is occupied by ions that enter the channel from side II and leave from either side. There is an irreversible transition from the state 1_b on side I to the empty state.

Let $s \in \{a, b\}$. P_i^s is the probability that the system is in state i_s. $C_s(x)$ is the concentration of ions of type s in the channel. Probabilities and concentrations are related by

$$P_i^s = C_i^s AL/n, \tag{31}$$

where $C_i^s = C_s(x_i)$ with $x_i = i/n$.

Transition probabilities are given by Eqs. 8–13 without modification. Under steady-state conditions, the state probabilities within cycle s are related by

$$P_i^s(\gamma_i + \hat{\gamma}_i) = P_{i-1}^s\gamma_{i-1} + P_{i+1}^s\hat{\gamma}_{i+1}. \tag{32}$$

Entrance and exit from cycle a are governed by the following relationships between state probabilities:

$$P_1^a(\gamma_1 + \beta_I) = P_2^a\hat{\gamma}_2 + P_E\alpha_I C_I, \tag{33}$$

$$P_n^a(\hat{\gamma}_n + \beta_{II}) = P_{n-1}^a\gamma_{n-1}, \tag{34}$$

with no term corresponding to the entrance of ions from side II. In contrast, entrance and exit from cycle b are governed by

$$P_1^b(\gamma_1 + \beta_I) = P_2^b\hat{\gamma}_2, \tag{35}$$

$$P_n^b(\hat{\gamma}_n + \beta_{II}) = P_{n-1}^b\gamma_{n-1} + P_E\alpha_{II}C_{II}, \tag{36}$$

with no term corresponding to entrance of ions from side I.

Equation 32 for ion movement in the interior of each cycle is analyzed in the same way as Eq. 16. We substitute in the definitions for the transition probabilities, simplify, let $n \to \infty$, and integrate twice to obtain

$$J_s h(x) = -ADL^{-1}[C_s(x)e^{v(x)} - C_s(0)e^{v(0)}], \tag{37}$$

with $h(x)$ given by Eq. 22 and $s \in \{a, b\}$. J_a is the unidirectional flux of ions from side I to side II, and J_b is the unidirectional flux from side II to side I.

We substitute the definitions for the transition probabilities into the entrance and exit relationships for cycle a, Eqs. 33 and 34, simplify, let $n \to \infty$, and make use of the Nernst-Planck equation (Eq. 1) to obtain boundary conditions for cycle a:

$$C_a(0) - P_E e^{\psi(1)-v(0)}C_I + \kappa_I(L/AD)J_a = 0, \tag{38}$$

$$C_a(1) - \kappa_{II}(L/AD)J_a = 0. \tag{39}$$

A similar analysis of the entrance and exit relationships for cycle b, Eqs. 35 and 36, yields the boundary conditions

$$C_b(0) + \kappa_I(L/AD)J_b = 0, \tag{40}$$

$$C_b(1) - P_E e^{-v(1)}C_{II} - \kappa_{II}(L/AD)J_b = 0. \tag{41}$$

The limiting process takes a sequence of random walks, the nth member of which is depicted in Fig. 2 *B*, to a diffusion process on a continuous-state diagram with two directed cycles, shown in Fig. 2 *D*. The empty state E serves as the boundary for both cycles. Arrows indicate irreversible transitions from the cycles to the empty state.

To see that Eqs. 37–41 are equivalent to the one-cycle analysis of the modified Levitt theory, we define $C(x) = C_a(x) + C_b(x)$ and $J = J_a + J_b$. Then we simply add the versions of Eq. 37 for $s = a$ and $s = b$ to get precisely Eq. 21. We add Eqs. 38 and 40 to get the one-cycle boundary condition on side I, Eq. 5. Finally, we add Eqs. 39 and 41 to get the one-cycle boundary condition on side II, Eq. 6. The modified Levitt theory follows from these equations.

In 1949, Ussing showed that the independence of the unidirectional fluxes J_a and J_b implied that the ratio of their magnitudes had the value

$$\frac{|J_a|}{|J_b|} = e^{\Delta\mu} = \frac{C_I}{C_{II}}e^{\psi_I}, \tag{42}$$

where $\Delta\mu$ is the dimensionless chemical potential difference across the membrane. This result would be expected, for example, if ion transport across the membrane took place by diffusion across the bulk of the membrane. In 1955, Hodgkin and Keynes reported the measurement of K^+ flux ratios transported across the membrane of the squid giant axon. Their results were not consistent with Eq. 42, but were well described by $|J_a|/|J_b| = \exp n'\Delta\mu$, where n' is called the flux ratio exponent. Hodgkin and Keynes found that $n' \approx 2.5$ best fit their measurements. This analysis of the K^+ flux across the squid giant axon initiated a large

literature concerned with multi-ion conduction (reviewed by Hille, 1992).

The development of the modified Levitt theory based on the directed two-cycle diagram allows us to calculate the flux ratio exponent for the present single-ion theory. We form an expression for $C_a(1) \exp v(1) - C_a(0) \exp v(0)$ from Eqs. 38 and 39 and insert the result into Eq. 37, evaluated at $x = 1$. We solve for the unidirectional flux to obtain

$$J_a = P_E(AD/L)C_I e^{\psi_I} f^{-1}, \quad (43)$$

where f is given by Eq. 26. A similar analysis based on Eq. 37 for $s = b$ and Eqs. 40 and 41 yields

$$J_b = -P_E(AD/L)C_{II} f^{-1}. \quad (44)$$

Dividing, we see that the ratio of the unidirectional fluxes obeys the independence principle (Eq. 42). This result is similar to that of Läuger (1973), who developed a theory of single-ion transport based on a discrete state model and also found $n' = 1$. The only coupling between the unidirectional fluxes in either of these single-ion theories is through the occupancy of the empty state, and this does not lead to a violation of the independence principle.

Description of the simulation programs

In Results we illustrate the difference between the Levitt and modified theories by presenting simulated ion trajectories at the channel entrances. In this section, we describe how the simulation programs work and compare the simulations with exact results.

Our programs simulate the discrete-time, discrete-state random walk based on the directed two-cycle diagram shown in Fig. 2 *B* and analyzed in the previous section. An ion that originally enters the channel from side I (that is, makes a transition from the state E to the state 1_a) can thereafter enter or exit the channel reversibly from side I, but makes an irreversible transition out of the channel on side II. Similarly, an ion that originally enters the channel from side II (from state E to state n_b) makes an irreversible transition out of the channel on side I. To compute currents, an ion is counted as having translocated the channel when it makes an irreversible transition to the empty state.

To simulate ion movement in the interior of the pore, we make direct use of the transition probabilities (Eqs. 8–13). The single value of $\Delta\tau$ (Eq. 14) is chosen so that the probability of making a transition out of any state in the random walk does not exceed 1. A uniform random number is generated and used to determine the ion's movement according to the transition probabilities γ_i, $\hat{\gamma}_i$, β_I, or β_{II}. For the examples in this paper, the simulations were run on a DEC 3000 model 400 workstation, performing about 10^9 time steps per hour.

Under typical conditions, and for a given time step, the probability of ion movement in an occupied channel is much larger than the probability of ion entrance into an empty channel. Instead of cycling many times through the time step loop in the empty state, channel entry is computed in the following manner. A uniform random number is generated and used to choose a random duration in the empty state according to the appropriate geometric distribution (see Results). A second random number determines the side of the channel through which the ion will enter. As a result, the computation is made much more efficient, especially when C_I and C_{II} are small or κ_I and κ_{II} are relatively large.

Fig. 3 compares probability densities $ALC(x)$ generated by the simulation of $n = 200$ and $n = 1000$ random walks with that obtained by exact integration of the modified Levitt solution (Eq. 27). The example was constructed using the intrinsic potential $\phi(x)$ specified by the 4-Å Jakobsson, Chiu, and Jordan (JCJ) potential profile with the $D = 2.0\ 10^{-10}\ m^2\ s^{-1}$ parameters listed in Table 1. The JCJ profiles are described in the Results. Fig. 6 *A* shows two examples. They are piecewise linear, interpolating between given points at 1-Å intervals.

The exact integration shown in Fig. 3 is obtained by a procedure similar to that described by Jakobsson and Chiu (1987). The integrals in Eq. 27 are performed analytically, and the computer only evaluates the resultant expressions. Under the conditions of Fig. 3, the empty probability $P_E = 0.498$.

The exact result is compared with those generated by the simulation program. Both simulations were run for 100 μs

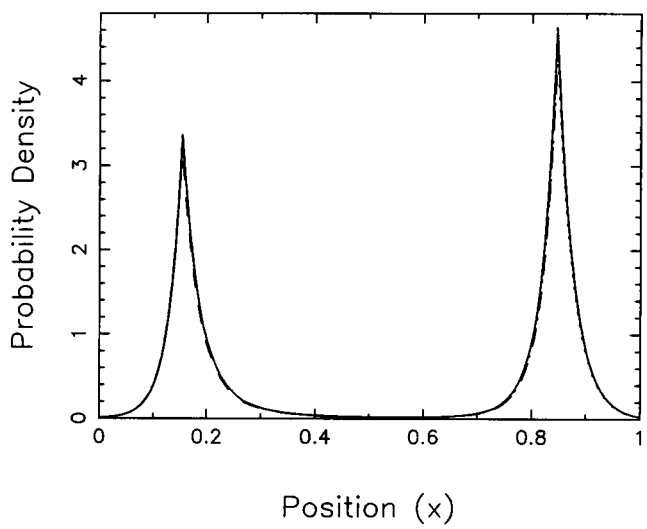

FIGURE 3 Simulated and exact modified Levitt theory probability densities. The ordinate is the probability density $ALC(x)$, and the abscissa is the axial location of the ion. Areas under the curves give the occupation probability $1 - P_E$. Curves are generated using the 4-Å JCJ potential profile with the $D = 2.0 \times 10^{-10}\ m^2\ s^{-1}$ parameters listed in Table 1. Bulk ion concentrations are $C_I = C_{II} = 200$ mM, and the transmembrane potential is $\Psi_I = 100$ mV. The discontinuous slope of the probability densities reflects the piecewise linear intrinsic potential. (*Solid curve*) Exact piecewise linear integration of modified Levitt theory. (*Dotted curve*) Probability density generated from 100 μs of simulated time with $n = 1000$ states along the pore (about 6×10^9 time steps). (*Dashed curve*) Probability density generated from 100 μs of simulated time with $n = 200$ states along the pore (about 244×10^6 time steps).

TABLE 1 Summary of 4-Å JCJ analysis

Diffusion coefficient D^*	Entrance potential ζ $(kT)^\#$	Well energy ϵ $(kT)^\#$	Barrier height η $(kT)^\#$	Binding kinetics κ	MSFE 10^{-4}	$\bar{\Phi}$ $(kT)^\#$
0.74	0	−5.29	4.10	0	9.28	−3.42
1.0	0	−5.38	4.54	0.010	7.37	−3.43
2.0	0	−5.55	5.48	0.049	5.62	−3.46
5.0	0	−5.70	6.62	0.163	5.00	−3.48
10.0	0	−5.78	7.45	0.355	4.85	−3.49
15.0	0	−5.82	7.92	0.543	4.80	−3.49

$^*10^{-10}$ m^2 s^{-1}.
$^\#T$ = 298 K.

of simulated time. Simulated densities are seen to be very similar to the exact result. The empty probability computed for $n = 200$ is 0.515 ± 0.020, whereas that computed for $n = 1000$ is 0.512 ± 0.012. To compute the errors, the simulated trajectories were divided into 10 blocks of equal length. The error given is twice the sample standard deviation of the mean.

We have also examined the convergence of the simulated conductances to exact results. For the modified Levitt simulation shown in Fig. 3, with $n = 1000$, the simulated conductance is 99.4 ± 9.0% of the exact value. In the case of $n = 200$, the simulated conductance is 97.5 ± 7.5% of the exact. Errors are again twice the sample standard deviation of the mean. Conductances computed from simulations of the original Levitt theory give a similar close comparison with those exact values.

RESULTS

We shall first characterize the difference between the boundary conditions of the Levitt (Eqs. 3 and 4) and modified Levitt (Eqs. 5 and 6) theories. These will then be used to calculate conductances using free energy profiles for Na^+ in gramicidin that have previously been described (Jordan, 1982; Jakobsson and Chiu, 1987; Åqvist and Warshel, 1989; Roux and Karplus, 1993). Finally, a formula will be derived relating the binding kinetics parameter κ to more familiar quantities in the special case of diffusion-limited ion entrance into the pore.

For simplicity, in these results, we shall assume that there is no applied potential drop in the electrolyte solution outside the channel, $\psi(0) = \psi_I$ and $\psi(1) = 0$. Furthermore, we suppose that the membrane/channel system is symmetrical, $\kappa_I = \kappa_{II} = \kappa$, and that $\phi(0) = \phi(1) = \zeta$. The qualitative features of the comparison between Levitt and modified Levitt theory boundary behaviors presented in the next two subsections hold in the general case.

Empty-state dwell times

How do the boundary conditions of the modified Levitt theory (Eqs. 5 and 6) compare with those originally proposed by Levitt (Eqs. 3 and 4) as a model of ion entrance and exit? We begin to address the question by calculating the distribution of dwell times in the empty state for the two theories.

First, consider the random walk pictured in Fig. 2 *A*, with finite n. Suppose that an ion exits the model channel, which is then initially in the empty state at a given time t_0. The probability that an ion will enter the channel on the next time step is P_{enter}, the sum of the probabilities of entrance from side I and side II,

$$P_{enter} = \alpha_I C_I + \alpha_{II} C_{II}. \tag{45}$$

As long as the channel remains in the empty state, P_{enter} remains the same for each successive time step. The probability that the channel will remain in the empty state for the next m time steps and that an ion will then enter the channel at time $t_0 + (m + 1)\Delta t$ is given by $(1 - P_{enter})^m P_{enter}$. The mean number of time steps $\bar{m}$ that the channel will continue to remain in the empty state is given by

$$\bar{m} = \sum_{m=0}^{\infty} m(1 - P_{enter})^m P_{enter} = P_{enter}^{-1} - 1. \tag{46}$$

The mean duration of the empty state, including the initial time step, is

$$\bar{T} = (\bar{m} + 1)\Delta t = \Delta t / P_{enter}. \tag{47}$$

Explicit expressions for the mean duration are obtained by substituting Eq. 45 and definitions of α_I and α_{II} into this formula for $\bar{T}$. In the case of the modified Levitt theory, α_I and α_{II} are given by Eqs. 10 and 11. The mean dwell time in the modified Levitt theory empty state is then

$$\bar{T}_{MLT} = \frac{L\kappa e^{\zeta}}{AD(C_I + C_{II})}. \tag{48}$$

This expression does not depend on n and remains fixed in the diffusion limit $n \to \infty$.

In the case of Levitt's original theory, the definitions of α_I and α_{II} are given by Eqs. 60 and 61. The mean duration of the Levitt empty state is then

$$\bar{T}_{Levitt} = \frac{L\kappa e^{\zeta}}{nAD(C_I + C_{II})}. \tag{49}$$

There is an additional factor of n in the denominator of $\bar{T}_{Levitt}$, when compared with $\bar{T}_{MLT}$. As a result, $\bar{T}_{Levitt} \to 0$ as $n \to \infty$.

Next, we calculate the distribution of empty-state dwell times in the modified Levitt theory. Let $p_{MLT}(t)$ be the probability that an interval in the empty state will have length of at least t. Consider first the random walk with a channel initially in the empty state at a given time t_0. Setting $t = m\,\Delta t$, the probability that the channel will remain empty for at least an additional time t is $(1 - P_{enter})^m$. To find $p_{MLT}(t)$, we must take the diffusion limit $n \to \infty$. Let $m \to$

∞ and $\Delta t = \Delta\tau/n^2 \rightarrow 0$ in such a way that their product t remains fixed. Then

$$p_{MLT}(t) = \lim_{m\to\infty}(1 - P_{enter})^m = \lim_{\Delta t\to 0}(1 - \Delta t/\bar{T}_{MLT})^{t/\Delta t} = e^{-t/\bar{T}_{MLT}}. \quad (50)$$

Dwell times in the modified theory empty state have exponentially distributed lengths.

This exponential distribution is a reasonable first approximation for the distribution of empty-state dwell times. It is the unique solution of the differential equation $dp/dt = -\bar{T}_{MLT}^{-1} p$, where $\bar{T}_{MLT}$ is independent of t, and $p(0) = 1$. Physically, this means that if the ion entry rate into an empty channel does not depend on the time elapsed since the channel became empty, dwell times in the empty state will be exponentially distributed. This conclusion does not depend on the detailed mechanism of ion entry. However, if channel degrees of freedom governing ion entrance relax on time scales comparable to the mean time in the empty state, use of the exponential distribution could be a poor approximation.

Behavior of ion trajectories near the channel entrance

We can better understand the implications of these results by examining sample ion trajectories generated by computer programs that simulate random walks in the sequence converging to the Levitt and modified theories. These programs are described in Methods and use transition probabilities for the Levitt theory (Eqs. 8, 9, and 60–63) or the modified theory (Eqs. 8–13).

Fig. 4 *A* shows trajectories for the $n = 500$ Levitt process. The pore lies in the interval $0 \leq x \leq 1$ on the ordinate, and the empty state is designated E below $x = 0$. Gaps in the empty state correspond to ion occupation of the pore. Two trajectories are shown crossing the pore, one in either di-

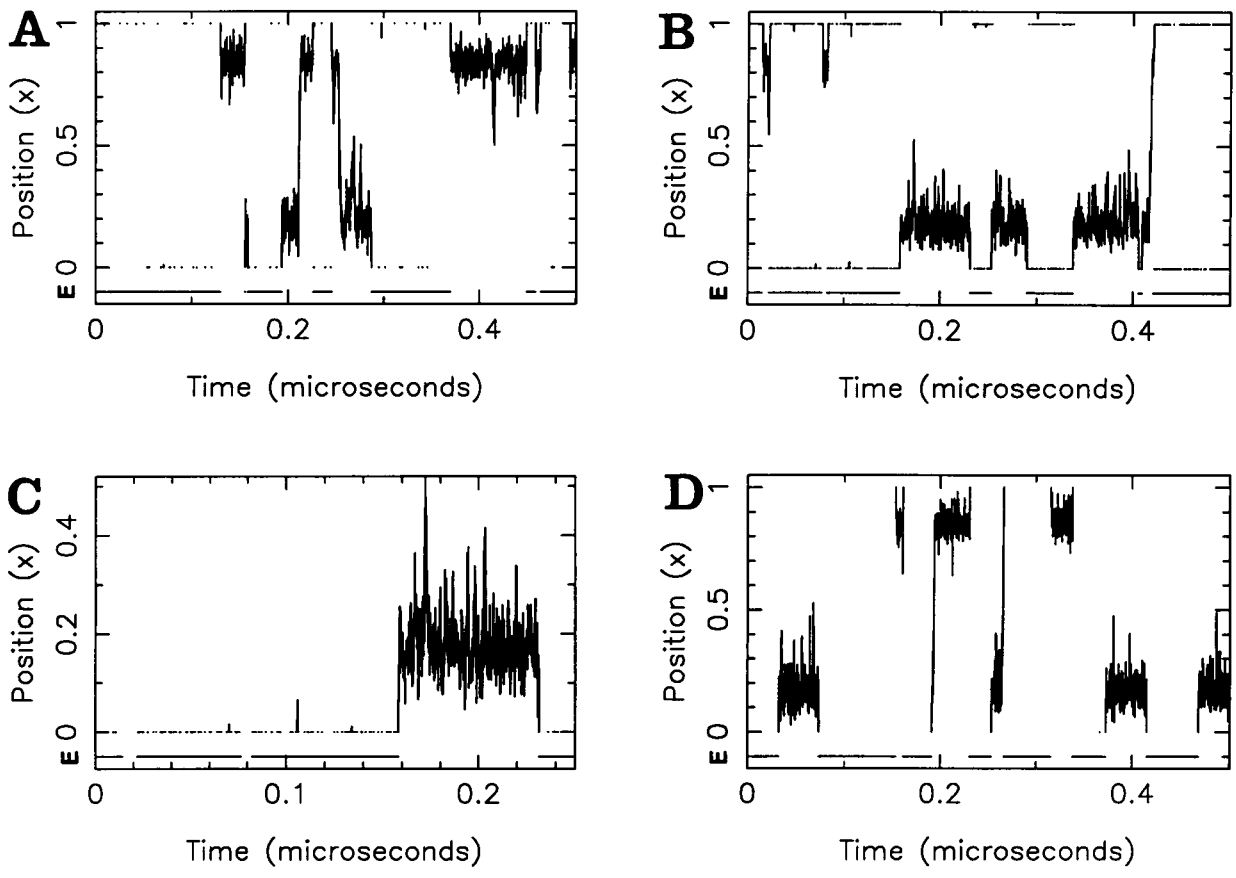

FIGURE 4 Levitt and modified Levitt theory trajectories. These figures show ion trajectories produced by the random walk simulation program. Time is on the abscissa, and axial location of the ion is on the ordinate. The state *E*, representing the empty channel, is shown separately under the states of the occupied pore. In each case, intrinsic potentials are 4-Å JCJ free energy profiles. Bulk ion concentrations are $C_I = C_{II} = 200$ mM, and the transmembrane potential is $\Psi_I = 100$ mV. $\Psi(x)$ is modeled as a linear ramp between the channel entrances. (*A*) Random walk simulation of Levitt theory with $n = 500$ states along the pore. Free energy profile parameter values are given by the line $D = 0.74\ 10^{-10}\ m^2\ s^{-1}$ in Table 1. Two trajectories cross the pore, one in each direction. (*B*) Simulation of Levitt theory with $n = 4000$. Note increased density of short-lived entrance events. (*C*) Detail of boundary behavior in *B*. (*D*) Simulation of modified theory with $n = 4000$. Free energy profile parameters are given by the line $D = 2.0 \times 10^{-10}\ m^2\ s^{-1}$ in Table 1. Compared to *B*, there are long quiescent intervals in the empty state. There are four short-lived entrances in the record, at 12, 13, 366, and 455 ns.

rection. Others enter and exit the pore from the same side of the channel. Among these latter trajectories are some that seem to briefly enter the pore and then immediately exit.

Fig. 4 *B* shows trajectories for the $n = 4000$ Levitt process. There are still significant intervals during which the deep interior of the pore is not occupied, but we see at these times an increase in the density of short-lived entrance events. These reflect the decreasing mean duration of the empty state, in accord with Eq. 49. Fig. 4 *C* is a detail of the lower left-hand corner of Fig. 4 *B*.

Fig. 4 *D* shows trajectories of the modified Levitt theory for $n = 4000$. The relatively long dwell times in the empty state reflect a finite mean duration in the limit $n \to \infty$, consistent with Eq. 48.

We summarize the description of the ion trajectories underlying Levitt's original boundary conditions (Eqs. 3 and 4). The mean dwell time in the empty state is zero. Despite this, the probability of the empty state is nonzero. Loosely speaking, we can characterize the occupation times of the empty state as a random fractal. Clearly, this is not physically realistic. There should be finite intervals of time during which the channel is always empty.

Conductance G_0 at symmetric equilibrium

Consider a symmetric channel, $\kappa_I = \kappa_{II} = \kappa$ and $\phi(0) = \phi(1) = \zeta$, embedded in a symmetric membrane with the same electrolyte solution on both sides. The concentration of the single permeant ion will be denoted $C_I = C_{II} = C_b$. We can use the result for the flux of the modified Levitt theory to compute an expression for the conductance at a symmetrical equilibrium. The current $\mathcal{J}$ is related to the flux by $\mathcal{J} = ze_0J$, where z is the permeant ion valence. From Eqs. 22, 25, 26, and 28 we obtain

$$G_0 = (\partial\mathcal{J}/\partial\Psi_I)_{\Psi_I=0,C_I=C_{II}=C_b} = (z^2e_0^2/kT)(AD/L)C_bP_Ef^{-1}, \quad (51)$$

where

$$P_E = \left[1 + ALC_b\int_0^1 e^{-\phi(x)}dx\right]^{-1}, \quad (52)$$

$$f = 2\kappa e^{\zeta} + \int_0^1 e^{\phi(x)}dx. \quad (53)$$

This expression is considerably simplified by the evaluation at a symmetrical equilibrium. Note that it is independent of $\psi(x)$, the function that describes the applied potential inside the channel. The difference between the Levitt and modified theories is due only to the term proportional to κ in the expression for f. The Levitt theory is obtained by taking $\kappa \to 0$.

G_0 has a Langmuir isotherm form when the concentration is considered an independent variable. The Michaelis constant is K_M, where

$$K_M^{-1} = AL\langle e^{-\phi}\rangle, \quad (54)$$

and $\langle e^{-\phi}\rangle$ symbolizes the integral appearing in Eq. 52. This form for K_M is already available in the Levitt theory (Levitt, 1986). Given values for K_M, A, and L, one can estimate $\langle e^{-\phi}\rangle$. Then define

$$\bar{\phi} = -\ln\langle e^{-\phi}\rangle. \quad (55)$$

$\bar{\phi} = \bar{\Phi}/kT$ is a weighted average of ϕ, where the more negative parts of the potential have exponentially greater influence.

Experimentally, G_0 must be estimated by current measurements at a small transmembrane potential. The data of Russell et al. shown in Fig. 5 *A* are based on current measurements at 25 and 50 mV (Russell et al., 1986). These give a value of $K_M = 165$ mM for the least-squares Langmuir Isotherm. Assuming that the channel has a diameter of 4 Å and a length of 26 Å, we find

$$\bar{\Phi}_{expt} = -3.43kT, \quad (56)$$

where the measurements took place at a temperature of $T = 298$ K.

Potential energy of Jakobsson, Chiu, and Jordan

In this section we will use the modified Levitt theory to analyze the gramicidin conductance data of Russell et al. (1986) using model intrinsic potentials similar to those of Jakobsson and Chiu (1987).

Jakobsson and Chiu (1987) considered potential profiles with 1-Å-wide entrance regions within which ϕ decreased linearly to potential energy minima 1 Å from the channel entrances. These two minima were separated by a scaled version of the electrostatic potential barrier computed by Jordan (1982). Conductances computed from this profile using the Levitt theory were compared with the data of Russell et al., and by this means optimal values of the well depth, barrier height, and channel diffusion coefficient were found. This pore model had a length of $L = 26$ Å, and thus the binding sites were 12 Å from the center of the channel.

However, a recent analysis by Woolf and Roux (1995) of the NMR measurements of Smith et al. (1990) on the Na^+-gramicidin complex suggests that the dominant Na^+ binding site in gramicidin is located about 9 Å from the center. We are thus motivated to consider six different families of potential profiles, with minima located 1–6 Å from the channel entrances.

We refer to these as the wÅ JCJ (Jakobsson, Chiu, and Jordan) profiles, where the entrance width w is the distance from the channel entrance to the nearest potential minimum. Examples of 1-Å and 4-Å JCJ potentials are shown in Fig. 6 *A*. Their structure includes an entrance region and a central barrier. The well depth ϵ and barrier height η are

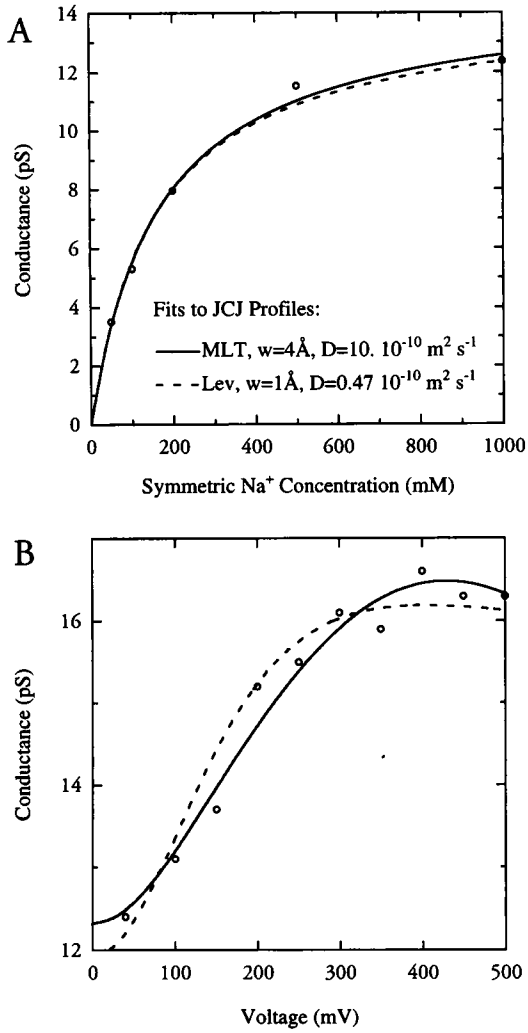

FIGURE 5 Levitt and modified Levitt theory fits to gramicidin conductance data of Russell et al. Fits are made to both of these data sets simultaneously. Solid curves represent the 4-Å JCJ modified Levitt theory fit with the parameters given by the line $D = 10 \times 10^{-10}$ m^2 s^{-1} shown in Table 1. Dashed curves represent the 1-Å JCJ Levitt theory fit with well depth $\epsilon = 5.22kT$, barrier height $\eta = 3.54kT$, and diffusion coefficient $D = 0.48\ 10^{-10}$ m^2 s^{-1}. Circles show conductance data. (*A*) Conductance as a function of concentration C_b. (*B*) Conductance as a function of applied transmembrane potential Ψ_I.

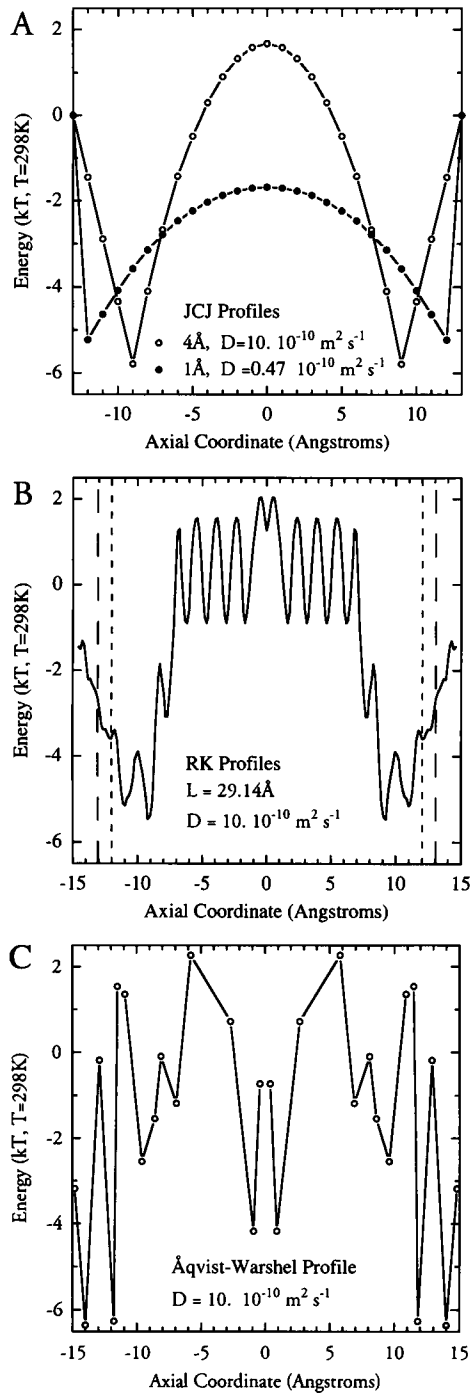

FIGURE 6 Potential energy profiles. (*A*) JCJ profiles. ●, Profile of the 1-Å JCJ Levitt theory fit to the conductance data of Russell et al., with parameter values given in the legend of Fig. 5. ○, Profile of the 4-Å JCJ modified Levitt theory fit with fixed $D = 10^{-10}$ m^2 s^{-1}. (*B*) RK profiles. The solid curve shows the full RK profile corresponding to $D = 10 \times 10^{-10}$ m^2 s^{-1}, the parameters of which are given in Table 2. Portions of the solid curve between the dashed or dotted lines are the two truncations considered in the text. (*C*) Åqvist and Warshel profile. This corresponds to $D = 10 \times 10^{-10}$ m^2 s^{-1}; parameters are given in Table 3.

defined in Fig. 1. All of the JCJ profiles have entrance potential $\zeta = 0$.

We will reanalyze the data of Russell et al., using both the Levitt and modified theories, to see how the optimal fits depend on the assumed entrance width. When using the Levitt theory, we followed Jakobsson and Chiu (1987) and optimized ϵ, η, and D. When using the modified theory, a value of D was fixed and ϵ, η, and κ were optimized.

Fig. 7 *A* shows results for each profile. The mean square fractional error (MSFE) of each fit to the combined data of Fig. 5 is plotted as a function of D. For each entrance width, the smallest value of D shown is that obtained from the Levitt analysis. For example, the Levitt fit shown by the dashed curves in Fig. 5 uses the 1-Å JCJ profile shown in Fig. 6 *A*. The resultant MSFE of 7.04×10^{-4} corresponds to an optimized value of $D = 0.47 \times 10^{-10}$ m^2 s^{-1}, the smallest diffusion coefficient in the family of 1-Å JCJ

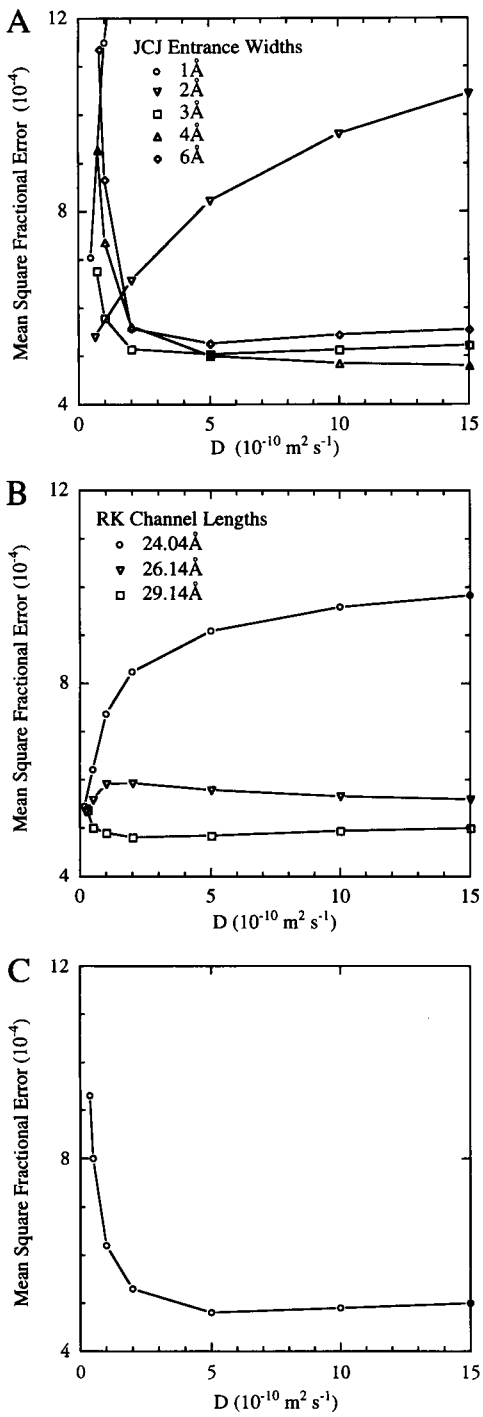

FIGURE 7 Mean fractional square errors as a function of D. Sets of fits using the same family of potential profiles are connected by straight lines. (*A*) Fits using the JCJ potentials. Within each set, the left-hand symbol corresponds to a Levitt theory fit with ϵ, η, and D optimized. Other symbols correspond to modified theory fits with D fixed and ϵ, η, and κ optimized. The 3-Å and 4-Å profiles give excellent fits to the data for a wide range of D. At each value of D, the MSFE for $w = 5$ Å is slightly higher than that for 4 Å. (*B*) Fits using the full and truncated RK potentials. Within each set, the left-hand symbol corresponds to the Levitt theory fit with σ, ζ, and D optimized. Other symbols correspond to modified theory fits with D fixed and σ, ζ, and κ optimized. The full RK potentials give excellent results. (*C*) Fits using the Åqvist-Warshel profile.

profiles. This result is shown as the left end point of the 1-Å MSFEs represented by the connected circles in Fig. 7 *A*. The modified Levitt fit shown by the solid curves in Fig. 5 uses the 4-Å JCJ profile shown in Fig. 6 *A*. The resultant MSFE of 4.85×10^{-10} corresponds to the value $D = 10 \times 10^{-10}$ m^2 s^{-1} fixed in the optimization. This result is represented by a triangle in Fig. 7 *A*.

The largest fixed value of the diffusion coefficient, $D = 15 \times 10^{-10}$ m^2 s^{-1}, is the value of the "fluid dynamic diffusion coefficient" found by Chiu et al. (1993) in a molecular dynamics simulation of the interior of the gramicidin pore. This is their estimated diffusion coefficient for the Na^+-water contents of gramicidin over small length scales. Chiu et al. conclude that it is an upper bound for the effective D we are concerned with here. Its value is approximately equal to the diffusion coefficient of Na^+ in water.

The results shown in Fig. 7 *A* are striking. The best fits for the 1-Å and 2-Å JCJ profiles are obtained using the Levitt theory. The 1-Å Levitt result is almost identical to that of Jakobsson and Chiu (1987). Modified Levitt fits using larger fixed values of D give markedly worse results. However, for profiles with entrance widths $w \geq 3$ Å, good fits are obtained for a broad range of values $D \geq 2 \times 10^{-10}$ m^2 s^{-1}. At each fixed value of D, the best fits are for profiles with $w = 3$ or 4 Å. These have binding site locations that are consistent with NMR results (Smith et al., 1990; Woolf and Roux, 1995).

Fig. 5 compares the Russell et al. data with conductances of the 1-Å JCJ Levitt theory fit, and with those of the 4-Å modified fit for $D = 10 \times 10^{-10}$ m^2 s^{-1}. The 4-Å JCJ profile yields a significantly better fit to the conductance-voltage data than the 1-Å JCJ profile.

The original Levitt theory fits the data best in the case of the 2-Å JCJ potential profile. This result is somewhat reminiscent of the refined analysis of the Russell et al. data given by Chiu and Jakobsson (1989). They added access resistance to the Levitt theory, but also modified the potential profile, effectively extending the width of the entrance regions to 2 Å. These changes resulted in an improved comparison with the experimental data.

Table 1 gives the parameter values, the MSFE, and calculated values of $\bar{\Phi}$ for the 4-Å JCJ fits shown in Fig. 7 *A*. Notice that $\kappa = 0$ at the smallest value of D, given by the Levitt analysis. Larger values of D are fixed for the modified analysis, and the optimized value of κ increases with D. Values of $\bar{\Phi}$ agree closely with those obtained directly from the data of Russell et al. (Eq. 56).

Modified Levitt theory fits of free energy profiles to the data of Russell et al. provide estimates of the mean dwell time of the channel in its empty state through Eq. 48. For example, the 4-Å JCJ parameters used to construct Fig. 4 *D* give $\bar{T}_{MLT} = 21$ ns. The sample mean dwell time of that simulation is about 27 ns, with short-lived channel entrances taken into account. $\bar{T}_{MLT}$ depends on the assumed value of D and κ. Assuming $C_I = C_{II} = 200$ mM, the free energy profile for $D = 1 \times 10^{-10}$ m^2 s^{-1} of Table 1 has

$\bar{T}_{MLT}$ = 9 ns, and that for $D = 10 \times 10^{-10}$ m^2 s^{-1} has $\bar{T}_{MLT}$ = 30 ns.

Potential energy of Roux and Karplus

In this section we use the modified Levitt theory to analyze the data of Russell et al. (1986) using scaled versions of the intrinsic potential calculated by Roux and Karplus (1993). Roux and Karplus computed an intrinsic energy profile for Na^+ occupation of gramicidin based on detailed molecular dynamics simulations of the gramicidin pore. Denote their original profile $U(\xi)$, where ξ is the distance in angstroms from the channel center and U has units of kT. Their tabulated profile extends to ξ_{max} = 14.57 Å. We arbitrarily define $U(\xi_{max}) = 0$.

$U(\xi)$ must be rescaled before it can be used to fit gramicidin conductance data. Consider a modified profile defined by

$$\Phi(x) = \sigma U(\xi) + \zeta kT, \tag{57}$$

where $x = (1 + \xi/\xi_{max})/2$. The pore extends over the interval $0 \le x \le 1$, corresponding to $-\xi_{max} \le \xi \le \xi_{max}$. We shall refer to the case of ξ_{max} = 14.57 Å as the full Roux-Karplus (RK) profile. Fig. 6 *B* shows Φ for particular values of σ and ζ.

The two new parameters that appear in Eq. 57 can be justified on physical grounds. The energy offset ζ gives an entrance potential $\phi(0) = \phi(1) = \zeta$. A nonzero value of ζ is physically reasonable because a sodium ion is still bound to two gramicidin oxygens, even at ξ = 14.95 Å, the furthest extent of the simulations. The zero energy is then defined by the limiting configuration when the sodium ion is far removed from the channel.

A coefficient σ is also required for a plausible attempt to fit the Russell et al. data. The difference between the highest and lowest energies of $U(\xi)$ is $23.3kT$, compared to typical values of 5 or $6kT$ found by fitting JCJ profiles to the data. Without σ, fits of $\phi(x)$ to these data would require enormous and unreasonable values of D.

We have fit the full RK potential to the data of Russell et al. using the Levitt and modified theories. For the analysis using the Levitt theory, σ, ζ, and D are optimized. When the modified theory is used, D is fixed and σ, ζ, and κ are optimized. In Fig. 7 *B*, the lowest curve gives the MSFE for the full RK potential. The results are excellent, comparable to the best achieved by use of the 4-Å JCJ profiles.

Table 2 shows parameter values, MSFEs, and values of $\bar{\Phi}$ for these analyses. For the parameter values to be comparable to those given in Table 1, we list ϵ and η, as well as ζ. ϵ is the most negative value of the potential, at ξ = 9.25 Å. η is the maximum difference between potential values and is related to σ by $\sigma = \eta/23.3kT$. Using L = 29.14 Å, we obtain $\bar{\Phi}_{expt} = -3.31kT$, instead of Eq. 56. The values of $\bar{\Phi}$ listed in Table 2 are in good agreement.

For the results given in Table 2 the maximum value of σ is only 0.35, corresponding to $D = 15.0 \times 10^{-10}$ m^2 s^{-1}.

TABLE 2 Summary of full RK analysis

Diffusion coefficient D*	Entrance potential ζ $(kT)^\#$	Well energy ϵ $(kT)^\#$	Barrier height η $(kT)^\#$	Binding kinetics κ	MSFE 10^{-4}	$\bar{\Phi}$ $(kT)^\#$
0.30	−3.07	−4.25	2.21	0	5.38	−3.29
0.5	−2.88	−4.60	3.22	0.085	5.01	−3.32
1.0	−2.58	−4.90	4.33	0.225	4.90	−3.34
2.0	−2.26	−5.11	5.33	0.413	4.81	−3.35
5.0	−1.80	−5.32	6.58	0.769	4.84	−3.35
10.0	−1.45	−5.45	7.48	1.160	4.94	−3.36
15.0	−1.23	−5.50	7.99	1.470	5.00	−3.35

*10^{-10} m^2 s^{-1}.
#T = 298 K.

That is, the peak-to-peak amplitude of the original Roux-Karplus profile must be decreased by a factor of about 3 or more to fit the data assuming reasonable values of D.

Values of the mean time in the empty state, given by Eq. 48, are comparable to those found for the JCJ profiles. Assuming $C_I = C_{II}$ = 200 mM, the free energy profile for $D = 1 \times 10^{-10}$ m^2 s^{-1} in Table 2 yields $\bar{T}_{MLT}$ = 15 ns, and the profile for $D = 10.0 - 10^{-10}$ m^2 s^{-1} yields $\bar{T}_{MLT}$ = 23 ns.

Roux and Karplus (1993) describe the interval 9.17 Å $\le \xi \le$ 14.57 Å as a transition region from single-file to bulk-like solvation. Therefore, two truncations of the Roux-Karplus potential are also considered. They use ξ_{max} = 12.02 Å and ξ_{max} = 13.07 Å, with the entire applied electric potential drop assumed to take place in the interval $-\xi_{max} \le \xi \le \xi_{max}$. The truncated profiles are fit to the Russell et al. data as described above. Resulting MSFEs are shown by the two upper curves in Fig. 7 *B*. The full RK profile clearly fits the data best.

Potential energy of Åqvist and Warshel

Åqvist and Warshel computed a free energy profile for Na^+ in gramicidin using the protein dipoles Langevin dipoles method (1989). Our profile was constructed from their table 1, with three supplementary points, at ξ = 8.1 Å, 9.6 Å, and 11.8 Å, the free energies of which were estimated from their Fig. 3 *A*. An intrinsic potential $\Phi(x)$ was then obtained by scaling this result using Eq. 57. Fig. 6 *C* shows an example. The Åqvist-Warshel profile differs from the JCJ and RK cases in that there is a region of relatively low free energy near the center ξ = 0. Other regions of low free energy are found only 1 to 3 Å from the channel entrances.

We fit the Åqvist-Warshel profile to the Russell et al. data using the Levitt and modified theories in the same manner as for the full RK profile. Fig. 7 *C* plots the mean fractional square errors as a function of D. The optimal modified Levitt theory profile obtained using $D = 10 \times 10^{-10}$ m^2 s^{-1} is shown in Fig. 6 *C*. Table 3 gives potential profile parameters, MSFEs, and values of $\bar{\Phi}$ for these analyses. Modified Levitt fits to the data for $D \ge 5 \times 10^{-10}$ m^2 s^{-1} are comparable to the best JCJ and RK analyses.

TABLE 3 Summary of Åqvist-Warshel analysis

Diffusion coefficient D^*	Entrance potential ζ $(kT)^\#$	Well energy ϵ $(kT)^\#$	Barrier height η $(kT)^\#$	Binding kinetics κ	MSFE 10^{-4}	$\bar{\Phi}$ $(kT)^\#$
0.36	−3.71	−4.81	3.04	0	9.32	−3.25
0.5	−3.74	−5.10	3.77	0.006	8.02	−3.25
1.0	−3.70	−5.56	5.13	0.022	6.23	−3.28
2.0	−3.58	−5.86	6.29	0.050	5.26	−3.29
5.0	−3.37	−6.14	7.66	0.113	4.80	−3.31
10.0	−3.18	−6.30	8.62	0.198	4.87	−3.32
15.0	−3.06	−6.38	9.16	0.270	5.01	−3.32

*10^{-10} m^2 s^{-1}.
#T = 298 K.

Mean dwell times in the Åqvist-Warshel empty state are much shorter than those found for the 4 Å JCJ or full RK profiles. Optimal parameter values for $D = 1 \times 10^{-10}$ m^2 s^{-1} give $\bar{T}_{MLT} = 0.5$ ns, while those for $D = 10 \times 10^{-10}$ m^2 s^{-1} give $\bar{T}_{MLT} = 0.7$ ns.

Binding kinetics κ for diffusion-limited ion entrance

The binding kinetics parameter κ emerged from the random walk construction of single-ion boundary conditions described in Methods. It is a parameter that changes the absolute rate of ion entrance and exit but does not alter their ratio. In this section we obtain a formula for κ, in terms of more familiar channel parameters, which applies under conditions of diffusion-limited ion entry into the channel.

Empty-state dwell times of the modified Levitt theory are exponentially distributed, with mean $\bar{T}_{MLT}$ given by Eq. 48. Consider the Poisson random process, comprising a succession of events separated by such exponentially distributed waiting times. The average number of events per unit time is $\bar{T}_{MLT}^{-1}$ (e.g., Feller, 1968). We can regard the entry of ions into an empty single-ion channel as a Poisson process until the reception of the first ion. We will find an expression for the flux into the channel using a diffusion argument and equate it with $\bar{T}_{MLT}^{-1}$.

We model the approach of ions from outside the channel entrance as radially symmetrical diffusion into a hemispherical sink of radius r_c, commonly called the capture radius. Let C_{eff} be the effective background concentration, perhaps an average concentration a few nanometers away from the entrance. Let D_{eff} be the effective diffusion coefficient. Solve the diffusion equation, $\nabla^2 C = 0$, with boundary conditions $C(r_c) = 0$ and $C(\infty) = C_{eff}$. The solution of this well-known problem (Hille, 1992) yields a diffusion-limited flux into the hemispherical sink of $2\pi r_c D_{eff} C_{eff}$, which we identify as the flux into the channel entrance.

Suppose that the intrinsic potential ϕ does not extend appreciably into the solution. Then set $C_{eff} = C_I$ or C_{II}, as appropriate. Assume that r_c and D_{eff} have common values on sides I and II. Then the total ion flux into the channel from the two entrances is $2\pi r_c D_{eff}(C_I + C_{II})$. Equating this to $\bar{T}_{MLT}^{-1}$, given by Eq. 48, we obtain

$$\kappa^{NC} = \frac{1}{2\pi}\frac{A}{Lr_c}\frac{D}{D_{eff}}e^{-\zeta}, \tag{58}$$

where NC signifies "no charge."

A different expression may be obtained by using a simple model for surface charge effects. We assume that the entrance potential ζ extends into the solution and is approximately constant over the region determining the diffusion-limited flux. Also suppose that local equilibrium in this region is not greatly perturbed by the flux through the channel. Then the background concentration of permeant ions will be proportional to Boltzmann factors, for example, $C_{eff} = C_I \exp(-\zeta)$. Setting the resultant total flux into the channel equal to $\bar{T}_{MLT}^{-1}$, we obtain

$$\kappa^{SC} = \frac{1}{2\pi}\frac{A}{Lr_c}\frac{D}{D_{eff}}, \tag{59}$$

where SC signifies "surface charge."

The difference between Eqs. 58 and 59 lies in the dependence of κ on the entrance potential ζ. Insert the expression for κ^{NC} into the definitions of the entrance and exit rate constants, Eqs. 10–13, with $\psi(0) = \psi_I$ and $\psi(1) = 0$. The effect of a negative entrance potential is now to slow ion exit from the channel. If instead the expression for κ^{SC} is substituted, the effect of a negative entrance potential is to speed ion entrance.

In fact, values of κ tabulated in Table 2 for the full RK potential are considerably greater than those given in Table 1 for the 4-Å JCJ potential. This difference is qualitatively consistent with the form of Eq. 58. This suggests that if the RK profile is roughly correct, its negative entrance potentials are to be associated (at least in part) with a decreased ion exit rate.

Equation 58 also sheds light on the decreasing values of κ obtained as the fixed value of D decreases in Tables 1–3. The decrease in κ may be partially reflected in the decreasing ratio D/D_{eff}. But this is not the whole explanation, because D tends toward a positive value as $\kappa \rightarrow 0$. The effective capture radius r_c must also be increasing.

We estimate the capture radius by solving Eq. 58 for r_c. Values of κ are obtained from Tables 1–3. Take $D_{eff} = 13.3 \times 10^{-10}$ m^2 s^{-1}, the aqueous diffusion coefficient of Na^+ (Hille, 1992). For the 4-Å JCJ profile we obtain $r_c = 0.16$ Å at $D = 10 \times 10^{-10}$ m^2 s^{-1}, increasing to $r_c = 0.58$ Å at $D = 1 \times 10^{-10}$ m^2 s^{-1}. Comparable results are obtained for the full RK profile, where $r_c = 0.19$ Å at $D = 10 \times 10^{-10}$ m^2 s^{-1}, increasing to $r_c = 0.30$ Å at $D = 1 \times 10^{-10}$ m^2 s^{-1}. In contrast, larger values of the effective capture radius are obtained from the fits of the Åqvist-Warshel profile to the data. These range from $r_c = 6.2$ Å at $D = 10 \times 10^{-10}$ m^2 s^{-1} up to $r_c = 17.8$ Å at $D = 1 \times 10^{-10}$ m^2 s^{-1}.

Andersen (1992) discusses the assumption of diffusion-limited entrance into a channel. Physically, one would ex-

pect this to overestimate the ion flux into the channel, because the channel is not a perfect sink. Equivalently, for a given entry rate into the channel, use of Eq. 58 should underestimate the capture radius. The values of r_c obtained from fits of the 4-Å JCJ and full RK profiles to the Russell et al. data seem compatible with this conclusion. However, the results obtained from fits of the Åqvist-Warshel profile stand out as anomalous.

DISCUSSION

Comparison of Levitt and modified theories

Our starting point is an attempt to understand the ion trajectories at the channel boundaries that underlie Levitt's (1986) single-ion diffusion theory. We construct a sequence of random walks, indexed by n, as shown in Fig. 2 *A*. States 1 through n represent ion occupation of the interior of the channel. Transition probabilities between these states, Eqs. 8 and 9, are chosen so that the Nernst-Planck equation (Eq. 1) is obtained in the limit $n \to \infty$. The empty channel is represented by the single additional state E. Boundary conditions for single ion diffusion depend on how the entrance and exit transition probabilities scale with n.

Two different scalings are considered. When entrance and exit rates are scaled by Eqs. 60–63, Levitt's boundary conditions, Eqs. 3 and 4, are obtained in the limit $n \to \infty$. However, this scaling has the peculiar property that the entrance rates $\alpha_I C_I$ and $\alpha_{II} C_{II}$ become infinite as n does. When entrance and exit rates are scaled by Eqs. 10–13, the modified Levitt boundary conditions, Eqs. 5 and 6, are obtained instead. In this case entrance rates remain finite as $n \to \infty$.

The behavior of the ion trajectories at the boundaries is studied by calculating the distribution of dwell times in the empty state E. A remarkable conclusion is reached. The mean time in the Levitt theory empty state is 0, even though the probability of that state is positive. This property is not physically appropriate. On the other hand, the mean time in the modified theory empty state is positive (Eq. 48), and those dwell times are distributed exponentially (Eq. 50).

These conclusions must be qualified. We have not proved that there is not another way to construct ion trajectories underlying Levitt's original theory. Conceivably, such an alternative set of trajectories could show more appropriate boundary behavior.

Physical trajectories of ions near channel entrances will have a more complicated structure than those that underlie the modified theory. As an ion leaves the channel, there may be a succession of brief entrances and exits followed by an interval in the empty state. However, such a fine structure of entrances and exits connected with the trajectory of a single ion will not have a significant effect on channel conductance.

A physical interpretation can be offered for the terms in the original Levitt boundary conditions (Eqs. 3 and 4) and the additional term found in the modified boundary conditions (Eqs. 5 and 6). The interpretation is clearest at low permeant ion concentrations, when $P_E \approx 1$. The original Levitt boundary condition is that the concentration of permeant ion at the channel entrance is in equilibrium with the aqueous solution outside the entrance. When a current is flowing, the decrease in ion free energy in the direction of current flow takes place entirely within the single-file domain of the channel.

The additional term in the modified boundary conditions shifts the permeant ion concentration at a channel entrance away from equilibrium with the aqueous solution on that side. The entrance and exit processes are now also associated with a free energy drop in the direction of net current flow.

Fits to the Na^+ conductance data

The modified Levitt theory has been applied to an analysis of three proposed free energy profiles for Na^+ in gramicidin (Jordan, 1982; Jakobsson and Chiu, 1987; Åqvist and Warshel, 1989; Roux and Karplus, 1993). Conductances computed from these profiles are compared with the data of Russell et al. (1986). The modified theory allows a relatively simple analysis to be made by assuming that dwell times in the empty state are exponentially distributed. Many details of the ion entrance and exit processes are then folded into the single parameter κ. In all cases, fits to the data involved the optimization of three parameters.

In addition to a free energy profile and a value for κ, our model includes a simple description for the applied electric field inside the pore. We have assumed a linear drop of the total applied potential between the channel entrances. In fact, the applied electric field in the pore will not be uniform. Assuming a cylindrical pore geometry, Jordan (1982) has shown that the applied field feathers near the channel entrances. Using the dimensions of gramicidin, he estimates that about 10% of the total potential drop occurs outside of the pore.

Interfacial polarization also decreases the total applied potential drop across the pore (Andersen, 1983). But this effect is negligible under the conditions of low transmembrane potential or high Na^+ concentration used in the experiments of Russell et al. (1986).

We have also assumed that the applied electric field acts on the full unit electrical charge of the Na^+ ion. In fact, polarization of the channel, and especially water dipoles, will reduce the effective valence of the ion (Roux and Karplus, 1993; Roux et al., 1995).

A striking feature of our results is an upper bound on the peak-to-peak amplitude of the free energy profile. Assuming that the diffusion coefficient of the ion in the channel is no greater than its value in aqueous solution, fits to the JCJ and RK profiles have a maximum peak-to-peak amplitude of about $8kT$. Fits to the Åqvist-Warshel profile admit slightly higher amplitudes, up to about $9kT$. This upper bound seems firm. It holds for both Levitt and modified theory fits and is consistent with the earlier findings of

Jakobsson and Chiu (1987) and Chiu and Jakobsson (1989). It contrasts sharply with the $23kT$ peak-to-peak amplitude of the original free energy profile tabulated by Roux and Karplus.

It is likely that overestimated free energy differences are due to important nonadditive effects of second-order ion-induced polarization (Roux, 1993; Roux et al., 1995; Roux, private communication) not included in the calculation of the free energy profile (Roux and Karplus, 1993). However, it is conceivable that the overestimated energies are symptomatic of an inadequate model for the dynamics of gramicidin. Elber et al. (1995) suggest that ion transport through gramicidin involves large-scale, coherent motion of the channel. Such large-scale motions might relax potential barriers and give a different potential profile.

A second result of our analysis addresses the location of the Na^+ binding sites. When the modified Levitt theory is used to compute conductances, variants of the JCJ profile that fit the data best have free energy minima within 10 Å or closer to the channel center. This is consistent with the recent analysis by Woolf and Roux (1995) of the NMR measurements by Smith et al. (1990), suggesting that Na^+ prefers to be about 9 Å from the center. In contrast, fits of the JCJ profiles to the Russell et al. data using the original Levitt theory are optimal for entrance widths of about 2 Å, corresponding to binding sites 11 Å from the center.

Our kinetic analysis of the Na^+ binding site location does depend on the general shape of the potential profile. Good fits to the data of Russell et al. can also be achieved using the Åqvist-Warshel profile, the free energy minima of which, at either end of the pore, are 11 Å or more from the channel center. However, this profile has a third region of relatively low Na^+ free energy near the center.

We also calculated the diffusion-limited capture radii, r_c, of the best fit free energy profiles. These should be upper bounds of true capture radii. Values of r_c calculated from the 4-Å JCJ and full RK fits were consistent, in the range of 0.16–0.6 Å, whereas values calculated from the Åqvist-Warshel profile were 6 Å or greater. The values obtained from the Åqvist-Warshel profile seem anomalously large.

In conclusion, the free energy profiles that fit the data best are either variants of the Jakobsson and Chiu (1987) profile, with entrance widths of 3 Å or greater, or scaled versions of the full profile tabulated by Roux and Karplus (1993). These profiles are somewhat similar, with a pair of free energy minima 9 or 10 Å from the channel center and a broad potential barrier of height $8kT$ or less in between.

Concentrations versus activities

We conclude with an observation on the issue of whether to use concentrations or activities when modeling conduction through ion channels. When the formula for the current J, Eq. 25, is evaluated at thermodynamic equilibrium, we see that C_I and C_{II} must be interpreted as activities. This is because the condition $J = 0$ is precisely the Nernst equation, and this refers to activities. However, when we analyzed the data of Russell et al. (1986) on the basis of activities instead of concentrations, significantly poorer fits to the data were obtained (unpublished observations; the relative merits of the potential profiles, however, remain the same).

A difference between concentration and activity results is easily understood. The activity coefficients for NaCl in the range of concentrations used by Russell et al. (1986) vary from 0.82 for $C_I = C_{II} = 50$ mM to 0.67 for $C_I = C_{II} = 1$ M. This is a variation of 20%.

But why is it better to analyze the data using concentrations rather than activities? When sufficient current runs through the channel to be measured, the description of the ion entrance step should include diffusion to the channel entrance. This is illustrated by the derivation for κ under diffusion-limited conditions. The flux density in this derivation is equal to $D_{eff}\nabla C$, where C is the spatially varying concentration in the aqueous convergence region and D_{eff} is the associated ion diffusion coefficient. This is Fick's law, and by definition C is concentration. The question is, how does D_{eff} vary with concentration? Robinson and Stokes (1965) tabulate measured diffusion coefficients of NaCl at $T = 298$ K for all of the concentrations used by Russell et al. This set of diffusion coefficients varies by only 2%. We thus interpret our result as evidence for the importance of diffusion to the channel mouth in the entrance step under the conditions of the experiments of Russell et al.

APPENDIX A: DIRECT DERIVATION OF THE LEVITT THEORY

This appendix demonstrates a direct derivation of Levitt's single-ion theory from a sequence of random walks, each with a state diagram of the form shown in Fig. 2 *A*. We begin by following the argument given in Methods. The first difference occurs in the definition of the transition probabilities. Those for ions moving in the interior of the pore, Eqs. 8 and 9, remain the same. However, probabilities associated with ion entrance into or exit from the channel are all increased by a factor of n,

$$\alpha_I = \Delta t A D L^{-1} n \kappa_I^{-1} e^{\psi_I - v(0)}, \tag{60}$$

$$\alpha_{II} = \Delta t A D L^{-1} n \kappa_{II}^{-1} e^{-v(1)}, \tag{61}$$

$$\beta_I = \Delta t D L^{-2} n^2 \kappa_I^{-1}, \tag{62}$$

$$\beta_{II} = \Delta t D L^{-2} n^2 \kappa_{II}^{-1}. \tag{63}$$

The relationships between state probabilities under steady-state conditions (Eqs. 16–18) are the same as for the modified theory.

The analysis of ion movement in the interior of the channel also repeats the procedure given in Methods, with the result given by Eqs. 21 and 22. However, the analysis of the equations relating state probabilities at the ends of the channel, Eqs. 17 and 18, is different. The entrance and exit transition probabilities considered here have all been multiplied by a factor of n. We can take the additional factor of n into account by making the replacements $\kappa_I^{-1} \rightarrow n\,\kappa_I^{-1}$ and $\kappa_{II}^{-1} \rightarrow n\,\kappa_{II}^{-1}$. Equation 23 yields the modified Levitt boundary condition on side I. Instead of that equation, we

now consider

$$(C_2 - C_1) + \frac{1}{2n}(C_1 v_1' + C_2 v_2') + (P_E e^{\psi_1 - v(0)} C_I - C_1)\kappa_I^{-1} = 0. \tag{64}$$

If we now let $n \to \infty$, only the last term on the right survives. We obtain Levitt's boundary condition for side I, Eq. 3. The boundary condition on side II, Eq. 4, is obtained in a similar way.

APPENDIX B: STATE-DEPENDENT DIFFUSION AND CROSS SECTION

This section generalizes the modified Levitt theory to include a state-dependent cross section, $A(x)$, and diffusion, $D(x)$. Consider a single permeant ion and the state diagram of Fig. 2 *A*. We assign state i of the random walk the spatial coordinate $x_i = i/n$. For a function $F(x)$ we will write $F_i = F(x_i)$, $1 \le i \le n$. For state-dependent A, the relationship between state probability and ion concentration is

$$P_i = C_i A_i L/n. \tag{65}$$

For ion movement in the interior of the channel we define, instead of Eqs. 8 and 9, the following transition probabilities:

$$\gamma_i = \frac{\Delta t}{2L^2 A_i}\left[n^2(A_i D_i + A_{i+1} D_{i+1}) - \frac{n}{2}(A_i D_i v_i' + A_{i+1} D_{i+1} v_{i+1}')\right], \tag{66}$$

$$\hat{\gamma}_i = \frac{\Delta t}{2L^2 A_i}\left[n^2(A_i D_i + A_{i-1} D_{i-1}) + \frac{n}{2}(A_i D_i v_i' + A_{i-1} D_{i-1} v_{i-1}')\right]. \tag{67}$$

Only minor modifications are required for the entrance and exit probabilities. From Eqs. 10 through 13, we replace $A \to A_1$ and $D \to D_1$ on side I, and replace $A \to A_n$ and $D \to D_n$ on side II.

Steady-state transition probabilities are still related by Eq. 16 in the interior of the channel and by Eqs. 17 and 18 at the channel boundaries. Consider transport in the interior of the channel. Substituting the above modified definitions for the transition probabilities into Eq. 16, we can multiply by a common factor and rearrange terms to get

$$\begin{aligned} 0 = n^2[&(C_{i+1}A_{i+1}D_{i+1} - 2C_iA_iD_i + C_{i-1}D_{i-1}A_{i-1}) \\ &- C_i(A_{i+1}D_{i+1} - 2A_iD_i + A_{i-1}D_{i-1}) \\ &+ (C_{i+1} - 2C_i + C_{i-1})A_iD_i] + \frac{n}{2}[C_i(A_{i+1}D_{i+1}v_{i+1}' - A_{i-1}D_{i-1}v_{i-1}') \\ &+ (C_{i+1}A_{i+1}D_{i+1}v_{i+1}' - C_{i-1}A_{i-1}D_{i-1}v_{i-1}') \\ &+ (C_{i+1} - C_{i-1})A_iD_iv_i']. \end{aligned} \tag{68}$$

Similar to the transition between Eqs. 19 and 20, we recognize finite difference approximations to first and second derivatives. Letting $n \to \infty$ and $i \to \infty$ so that $i/n \to x$, and then simplifying, we obtain

$$\frac{d}{dx}\left(\frac{A(x)D(x)}{L}\frac{dC}{dx} + \frac{A(x)D(x)}{L}v'(x)C(x)\right) = 0. \tag{69}$$

This is the time-independent Fokker-Planck equation for state-dependent A and D. Integrating once, we obtain the Nernst-Planck equation:

$$J = -\frac{A(x)D(x)}{L}\left(\frac{dC}{dx} + v'(x)C(x)\right). \tag{70}$$

This is the form considered by Levitt (1986). We multiply by an integrating factor and integrate to obtain

$$-LJH(x) = C(x)e^{v(x)} - C(0)e^{v(0)}, \tag{71}$$

where

$$H(x) = \int_0^x \frac{Le^{v(\xi)}}{A(\xi)D(\xi)}\,d\xi. \tag{72}$$

Substituting the modified transition probabilities (see Eqs. 66, 67 and below) into the steady-state condition (Eq. 17) on side I and simplifying, we obtain

$$\begin{aligned} &\frac{n}{2}(C_2 - C_1)(A_1D_1 + A_2D_2) + \frac{1}{4}(C_1 + C_2)(A_1D_1v_1' + A_2D_2v_2') \\ &\quad + A_1D_1(P_Ee^{\psi_1 - v(0)}C_I - C_1)\kappa_I^{-1} = 0. \end{aligned} \tag{73}$$

We let $n \to \infty$, divide by $A(0)D(0)$, and use Eq. 70 to obtain for side I

$$C(0) - P_Ee^{\psi_1 - v(0)}C_I + \kappa_I\frac{L}{A(0)D(0)}J = 0. \tag{74}$$

Starting from Eq. 18, a similar analysis yields the boundary condition for side II:

$$C(1) - P_Ee^{-v(1)}C_{II} - \kappa_{II}\frac{L}{A(1)D(1)}J = 0. \tag{75}$$

Combine the boundary conditions, Eqs. 74 and 75, to obtain an expression for $C(1)\exp v(1) - C(0)\exp v(0)$, and substitute this into the result of evaluating Eq. 71 at $x = 1$. Solving for J, we obtain

$$J = P_E(C_Ie^{\psi_1} - C_{II})F^{-1}, \tag{76}$$

where

$$F = \frac{L}{A(0)D(0)}e^{v(0)}\kappa_I + \frac{L}{A(1)D(1)}e^{v(1)}\kappa_{II} + H(1), \tag{77}$$

and $H(x)$ is defined by Eq. 72.

P_E remains to be determined. Starting from Eq. 71, substitute for $C(0)e^{v(0)}$ using Eq. 74 and for J using Eq. 76. Solve for C to obtain

$$C(x) = P_Ee^{-v(x)}\left[C_Ie^{\psi_1} - (C_Ie^{\psi_1} - C_{II})\cdot\left(\frac{L}{A(0)D(0)}e^{v(0)}\kappa_I + H(x)\right)\right]F^{-1}. \tag{78}$$

Inserting this result into

$$P_E = 1 - \int_0^1 LA(x)C(x)\,dx, \tag{79}$$

and solving for P_E, we find

$$P_E = \left[1 + C_I e^{\psi_I} \int_0^1 LA(x)e^{-v(x)}dx + (C_{II} - C_I e^{\psi_I})R\right]^{-1}, \quad (80)$$

where

$$R = \int_0^1 LA(x)e^{-v(x)}\left(\frac{L}{A(0)D(0)}e^{v(0)}\kappa_I + H(x)\right)F^{-1}dx. \quad (81)$$

This completes the solution for J and $C(x)$.

We have developed the modified Levitt theory for a variable cross section and diffusion coefficient, the general case originally considered by Levitt (1986). For true single-file diffusion, however, it may be most useful to regard the channel cross section A as effectively constant. Then the Nernst-Planck equation (Eq. 70) can be written in terms of $\mathcal{P}(x) = AC(x)$, a probability per unit length.

APPENDIX C: MODIFIED LEVITT THEORY FOR TWO PERMEANT IONS

In this appendix we will generalize the modified Levitt single-ion theory to consider two permeant ions. Designate the ion species a and b, and let $s \in \{a, b\}$ refer to either. Consider the random walk shown in Fig. 8. A cycle of states describing ion a in the channel and a cycle describing ion b in the channel are linked by a common empty state E.

Associated with each cycle are formulas for the transition probabilities that are similar to Eqs. 8–13, with the exception that we introduce separate values of the diffusion coefficient, D_s, the derivative of the total potential, $v_i^{s\prime}$, and the binding kinetics parameters, κ_I^s and κ_{II}^s. In the following, we will assume that the two permeant ions have the same valence, so that the total potential $v_s(x) = \phi_s(x) + \psi(x)$, with a single value of ψ_I applying to both ion species.

For each cycle, the relationships between state probabilities P_i^s and concentrations C_i^s are given by Eq. 31. At steady state, the state probabilities are related by two sets of equations with the form of Eqs. 16–18, one set for $s = a$ and the other for $s = b$. These equations are linked only by the probability P_E of the common state E.

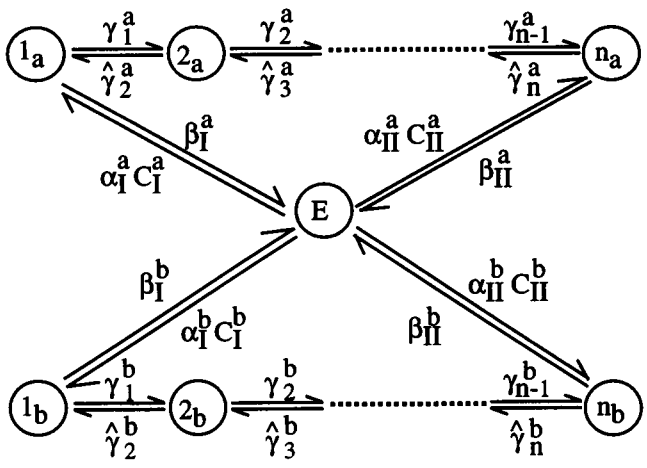

FIGURE 8 State diagram of modified Levitt theory with two permeant ions. The top cycle is occupied by ions of species a, and the bottom cycle is occupied by ions of species b. Symbols for transition probabilities are shown next to appropriate arrows. The two cycles are linked by the common empty state E.

Analysis of ion movement in the interior of each of the two cycles exactly parallels that for a single ion. The limit $n \to \infty$ leads to separate Fokker-Planck equations for ions a and b. These are integrated to give Nernst-Planck equations, which can be integrated again to obtain

$$J_s h_s(x) = -AD_s L^{-1}[C_s(x)e^{v_s(x)} - C_s(0)e^{v_s(0)}], \quad (82)$$

where

$$h_s(x) = \int_0^x e^{v_s(\xi)}d\xi. \quad (83)$$

The constants of integration are determined by boundary conditions that are developed from the equations for P_1^s and P_n^s. Parallel to the analysis for one permeant ion, these lead to

$$C_s(0) - P_E e^{\psi_I - v_s(0)}C_I^s + \kappa_I^s(L/AD_s)J_s = 0, \quad (84)$$

$$C_s(1) - P_E e^{-v(1)}C_{II}^s - \kappa_{II}^s(L/AD_s)J_s = 0, \quad (85)$$

for $s = a$ and $s = b$. Equations 82–85 are the result of a limiting process that takes a sequence of random walks (the nth member of which is depicted in Fig. 8) to a continuous-state diagram with two cycles, linked by the common state E. This could be depicted in a manner similar to that of Fig. 2 D, but with all transitions bidirectional.

We evaluate Eq. 82 at $x = 1$ and substitute for $C_s(x)\exp v_s(x) - C_s(0)\exp v_s(0)$ using the boundary conditions. Solve for the current J_s to obtain

$$J_s = P_E AD_s L^{-1}[C_I^s e^{\psi_I} - C_{II}^s]f_s^{-1}, \quad (86)$$

where

$$f_s = \kappa_I^s e^{v_s(0)} + \kappa_{II}^s e^{v_s(1)} + h_s(1). \quad (87)$$

To obtain expressions for the concentrations, consider Eq. 82. Substitute for $C_s(0)$ using Eq. 84 and for J using Eq. 86. Solve for $C_s(x)$ to get

$$C_s(x) = P_E e^{-v_s(x)}[C_I^s e^{\psi_I} - (C_I^s e^{\psi_I} - C_{II}^s)(\kappa_I^s e^{v_s(0)} + h_s(x))f_s^{-1}]. \quad (88)$$

An expression for P_E can be developed from the relationship

$$P_E = 1 - \int_0^1 ALC_a(x)dx - \int_0^1 ALC_b(x)dx. \quad (89)$$

Substitute the expression given by Eq. 88 for the concentrations and solve for P_E to obtain

$$P_E = \left[1 + C_I^a e^{\psi_I}\int_0^1 ALe^{-v_a(x)}dx + C_{II}^b e^{\psi_I}\int_0^1 ALe^{-v_b(x)}dx + (C_{II}^a - C_I^a e^{\psi_I})R_a + (C_{II}^b - C_I^b e^{\psi_I})R_b\right]^{-1}, \quad (90)$$

where

$$R_s = \int_0^1 ALe^{-v_s(x)}(\kappa_I^s e^{v_s(0)} + h_s(x))f_s^{-1}dx. \quad (91)$$

Eqs. 86–91 give a complete solution to the case for two permeant ions. The limits $\kappa_I^s \to 0$ and $\kappa_{II}^s \to 0$ for $s = a$ and $s = b$ lead to the Levitt single-ion theory in the presence of two permeant ions (Levitt, 1986).

This procedure can clearly be generalized to N permeant ions, starting with N cycles sharing a common empty state. State-dependent channel cross sections, $A(x)$, and diffusion coefficients, $D(x)$, can be incorporated by means of the procedure demonstrated in Appendix B.

APPENDIX D: SYMMETRIES OF THE REVERSAL POTENTIAL

In this section we show that the modified Levitt theory satisfies two qualitative symmetries that can serve to distinguish single-ion diffusion from multi-ion transport.

The reversal potential $\psi_I = \psi_R$ is a commonly measured property of conductance in the presence of two permeant ions. By definition, ψ_R is the applied electrical potential at which no net current flows through the channel. From the condition $J_a + J_b = 0$ and Eq. 86, we find that ψ_R is defined implicitly by

$$e^{\psi_R} = \frac{f_b D_a C_{II}^a + f_a D_b C_{II}^b}{f_b D_a C_I^a + f_a D_b C_I^b}. \tag{92}$$

Levitt (1986) obtained a similar equation. This is not an explicit solution, because f_a and f_b are themselves dependent on ψ_R.

In general, the intrinsic potential $\phi_s(x)$ may depend on the concentrations C_I^s and C_{II}^s. For example, entrance potentials may depend on surface charges, with the associated electrostatic potentials depending on ion concentrations outside the channel. Intrinsic potentials may also be dependent on ion concentrations through allosteric effects. When mechanisms like these are important, the factors f_s are dependent on concentrations (see Eq. 87). However, mechanisms like these may be insignificant.

Suppose that the intrinsic potentials ϕ_s do not depend on C_I^s and C_{II}^s. Then the factors f_s are independent of these concentrations and Eq. 92 is not changed if we rescale C_I^s and C_{II}^s, $s \in \{a, b\}$, by the same factor: $C_I^a \to \rho C_I^a$ and $C_{II}^b \to \rho C_{II}^b$. It follows that the solution ψ_R is independent of any such common factor ρ. In other words, the reversal potential is independent of absolute concentration. This qualitative property of the reversal potential of the Levitt and modified single-ion diffusion theories is also shared by single-ion theories based on discrete-state models (Läuger, 1973).

The reversal potential is often measured under bi-ionic conditions, that is, with one permeant ion on side I and the other permeant ion on side II. Let the symbol $[C_a \| C_b]$ represent the configuration $C_I^a = C_a$, $C_{II}^a = 0$, $C_I^b = 0$, and $C_{II}^b = C_b$. Under these conditions Eq. 92 becomes

$$e^{\psi_R} = \frac{f_a D_b C_{II}^b}{f_b D_a C_I^a} \tag{93}$$

Still assuming that the intrinsic potentials do not depend on concentrations, the bi-ionic reversal potentials of the Levitt and Modified single-ion diffusion theories satisfy another qualitative property of interest when the channels have asymmetrical intrinsic potentials (e.g., Garber, 1988). Consider again the configuration $[C_a \| C_b]$ and suppose that C_a and C_b are adjusted so that $\psi_R = 0$. From Eq. 93 it follows that

$$C_a/C_b = (f_a D_b)/(f_b D_a). \tag{94}$$

Now consider the configuration $[C_b \| C_a]$; that is, $C_I^a = 0$, $C_{II}^a = C_a$, $C_I^b = C_b$, and $C_{II}^b = 0$. The condition that $\psi_R = 0$ again leads to Eq. 94. In other words, if particular values of C_a and C_b are chosen so that $\psi_R = 0$ in the configuration $[C_a \| C_b]$, then we will also have $\psi_R = 0$ in the configuration $[C_b \| C_a]$. This symmetry is called orientation independence of the bi-ionic permeability ratio at $\psi_R = 0$, and it holds even though $\phi_a(x)$ and $\phi_b(x)$ may themselves be quite asymmetrical, or κ_I and κ_{II} much different. Orientation independence is also a property of both single-ion and single-vacancy theories based on discrete-state models (McGill and Schumaker, 1995).

We thank Eric Jakobsson for his introduction to the problem of ion permeation through gramicidin, and for sharing with us his Brownian dynamics simulation programs. We have also benefitted greatly from discussions and communications with Olaf Andersen, Peter Jordan, David Levitt, and Benoit Roux. Dr. Andersen kindly reviewed the manuscript. Verne Schumaker suggested that the concentration dependence of Na^+ entry into the channel would be determined in part by the concentration dependence of the Na^+ diffusion coefficient. We would also like to thank an anonymous referee for many helpful suggestions.

This work was supported by grant MCB 94-04430 from the National Science Foundation.

REFERENCES

Andersen, O. S. 1983. Ion movement through gramicidin A channels. Interfacial polarization effects on single-channel current measurements. *Biophys. J.* 41:135–146.

Andersen, O. S. 1992. Molecular determinants of channel function. *Physiol. Rev.* 72:S89–S158.

Åqvist, J., and A. Warshel. 1989. Energetics of ion permeation through membrane channels. *Biophys. J.* 56:171–182.

Chandrasekhar, S. 1943. Stochastic problems in physics and astronomy. *Rev. Mod. Phys.* 15:1–89.

Chiu, S.-W., and E. Jakobsson. 1989. Stochastic theory of single occupied channels. II. Effects of access resistance and potential gradients extending into the bath. *Biophys. J.* 55:147–157.

Chiu, S.-W., J. A. Novotny, and E. Jakobsson. 1993. The nature of ion and barrier crossings in a simulated ion channel. *Biophys. J.* 64: 98–109.

Cooper, K. E., P. Y. Gates, and R. S. Eisenberg. 1988. Diffusion theory and discrete rate constants in ion permeation. *J. Membr. Biol.* 106:95–105.

Cooper, K., E. Jakobsson, and P. Wolynes. 1985. The theory of ion transport through membrane channels. *Prog. Biophys. Mol. Biol.* 46: 51–96.

Dani, J. A., and D. G. Levitt. 1990. Diffusion and kinetic approaches to describe permeation in ionic channels. *J. Theor. Biol.* 146:289–301.

Elber, R., D. P. Chen, D. Rojewska, and R. Eisenberg. 1995. Sodium in gramicidin: an example of a permion. *Biophys. J.* 68:906–924.

Feller, W. 1968. An Introduction to Probability Theory and Its Applications. Wiley, New York.

Garber, S. 1988. Symmetry and asymmetry of permeation through toxin-modified Na^+ channels. *Biophys. J.* 54:767–776.

Gardiner, C. W. 1983. Handbook of Stochastic Methods. Springer-Verlag. Berlin.

Hille, B. 1992. Ionic Channels of Excitable Membranes, 2nd Ed. Sinauer Associates, Sunderland, MA.

Hille, B., and W. Schwarz. 1978. Potassium channels as multi-ion single-file pores. *J. Gen. Physiol.* 72:409–442.

Hodgkin, A. L., and R. D. Keynes. 1955. The potassium permeability of a giant nerve fiber. *J. Physiol. (Lond.).* 128:61–88.

Jakobsson, E., and S.-W. Chiu. 1987. Stochastic theory of ion movement in channels with single-ion occupancy. *Biophys. J.* 52:33–45.

Jordan, P. C. 1982. Electrostatic modelling of ion pores. *Biophys. J.* 39:157–164.

Karlin, S., and H. M. Taylor. 1981. A Second Course in Stochastic Processes. Academic Press, New York.

Läuger, P. 1973. Ion transport through pores: a rate theory analysis. *Biochim. Biophys. Acta.* 311:423–441.

Levitt, D. G. 1986. Interpretation of biological ion channel flux data: reaction rate versus continuum theory. *Annu. Rev. Biophys. Biophys. Chem.* 15:29–57.

McGill, P., and M. F. Schumaker. 1995. Orientation independence of single-vacancy and single-ion permeability ratios. *Biophys. J.* 69:84–93.

Reif, F. 1965. Fundamentals of Statistical and Thermal Physics. McGraw-Hill, New York.

Risken, H. 1989. The Fokker-Planck Equation. Springer-Verlag, Berlin.

Robinson, R. A., and R. H. Stokes. 1965. Electrolyte Solutions. Butterworths, London.

Roux, B. 1993. Non-additivity in cation-peptide interactions. A molecular dynamics and ab initio study of Na^+ in the gramicidin channel. *Chem. Phys. Lett.* 212:231–240.

Roux, B., and M. Karplus. 1993. Ion transport in the gramicidin channel: free energy of the solvated right-hand dimer in a model membrane. *J. Am. Chem. Soc.* 115:3250–3262.

Roux, B., B. Prod'hom, and M. Karplus. 1995. Ion transport in gramicidin: molecular dynamics studies of single and double occupancy. *Biophys. J.* 68:876–892.

Russell, E. W. B., L. B. Weiss, F. I. Navetta, R. E. Koeppe, II, and O. S. Andersen. 1986. Single-channel studies on linear gramicidins with altered amino acid side chains. *Biophys. J.* 49:673–686.

Smith, R., D. E. Thomas, A. R. Atkins, F. Separovic, and B. A. Cornell. 1990. Solid-state ^{13}C-NMR studies of the effects of sodium ions on the gramicidin A ion channel. *Biochim. Biophys. Acta.* 1026:161–166.

Ussing, H. H. 1949. The distinction by means of tracers between active transport and diffusion. *Acta Physiol. Scand.* 19:43–56.

Woolf, T. B., and B. Roux. 1995. Binding sites for sodium in gramicidin A: comparison of molecular dynamics calculations and solid-state NMR data. *Biophys. J.* 68:A150.